Elsevier Editorial System(tm) for Applied Thermal Engineering
Manuscript Draft

Manuscript Number: ATE-2010-714R1

Title: A Strategy for the Economic Optimization of Combined Cycle Gas Turbine Power Plants by Taking Advantage of Useful Thermodynamic Relationships

Article Type: Research Paper

Keywords: thermodynamic optimization; economic optimization; combined cycle power plants; optimal relationships

Corresponding Author: Dr. Nicolás J. Scenna, Ph.D

Corresponding Author's Institution: CAIMI - FRRo - UTN

First Author: Ezequiel Godoy, Chemical Engineer

Order of Authors: Ezequiel Godoy, Chemical Engineer; Sonia J Benz, Ph.D.; Nicolás J. Scenna, Ph.D

Abstract: Optimal combined cycle gas turbine power plants characterized by minimum specific annual cost values are here determined for wide ranges of market conditions as given by the relative weights of capital investment and operative costs, by means of a non-linear mathematical programming model. On the other hand, as the technical optimization allows identifying trends in the system behavior and unveiling optimization opportunities, selected functional relationships are obtained as the thermodynamic optimal values of the decision variables are systematically linked to the ratio between the total heat transfer area and the net power production (here named as specific transfer area).
A strategy for simplifying the resolution of the rigorous economic optimization problem of power plants is proposed based on the economic optima distinctive characteristics which describe the behavior of the decision variables of the power plant on its optima. Such approach results in a novel mathematical formulation shaped as a system of non-linear equations and additional constraints that is able to easily provide accurate estimations of the optimal values of the power plant design and operative variables.

Cover Letter

To: Editor of Applied Thermal Engineering Journal

Subject: Submission of manuscript of the paper "A Strategy for the Economic Optimization of Combined Cycle Gas Turbine Power Plants by Taking Advantage of Useful Thermodynamic Relationships"

Dear Sir,

Please find annexed with this letter the revised version of the manuscript of the paper "A Strategy for the Economic Optimization of Combined Cycle Gas Turbine Power Plants by Taking Advantage of Useful Thermodynamic Relationships" for revision and, if accepted, publication in the Applied Thermal Engineering Journal.

The authors state that this paper has not been published previously, it is not under consideration for publication elsewhere, and if accepted it will not be published elsewhere in substantially the same form, in English or in any other language, without the written consent of the Publisher.

I look forward to hearing from you.

Yours sincerely

Nicolás J. Scenna

Corresponding Author Contact Information

Affiliation: Centro de Aplicaciones Informáticas y Modelado en Ingeniería (CAIMI) - Universidad Tecnológica Nacional (UTN)

E-mail: nscenna@santafe-conicet.gov.ar

Postal Address: Zeballos 1346, 2º Piso – S2000BQB Rosario, Argentina

Telephone: +54 341 4484909 – int. 144

Graphical Abstract

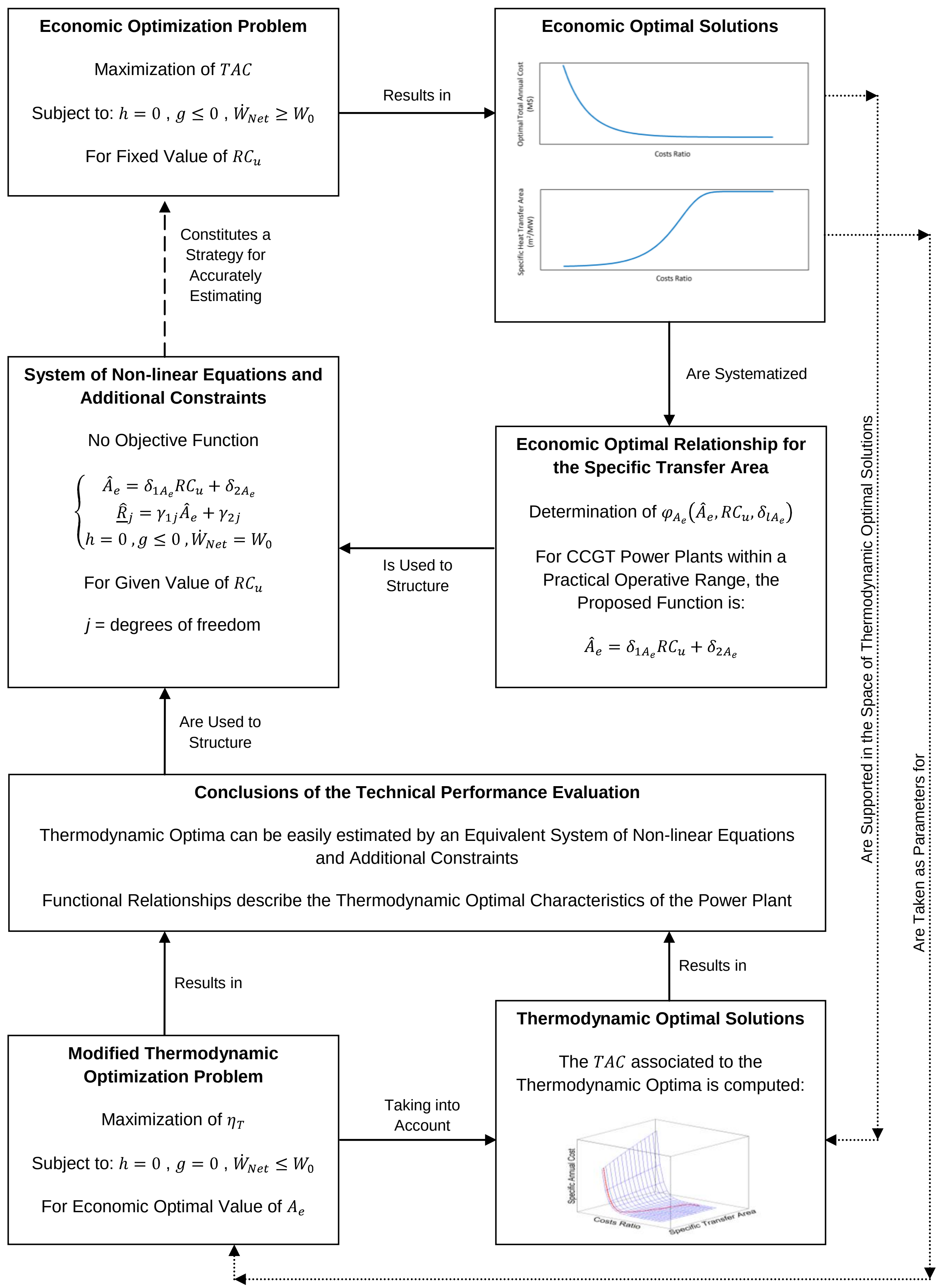

A Strategy for the Economic Optimization of Combined Cycle Gas Turbine Power Plants by Taking Advantage of Useful Thermodynamic Relationships

Godoy E.[1], Benz S. J.[1], Scenna N. J.[1,2]

[1]Centro de Aplicaciones Informáticas y Modelado en Ingeniería,
Facultad Regional Rosario, Universidad Tecnológica Nacional, Rosario, Argentina
[2]INGAR/CONICET, Instituto de Desarrollo y Diseño, Santa Fe, Argentina

Abstract:

Optimal combined cycle gas turbine power plants characterized by minimum specific annual cost values are here determined for wide ranges of market conditions as given by the relative weights of capital investment and operative costs, by means of a non-linear mathematical programming model.

On the other hand, as the technical optimization allows identifying trends in the system behavior and unveiling optimization opportunities, selected functional relationships are obtained as the thermodynamic optimal values of the decision variables are systematically linked to the ratio between the total heat transfer area and the net power production (here named as specific transfer area).

A strategy for simplifying the resolution of the rigorous economic optimization problem of power plants is proposed based on the economic optima distinctive characteristics which describe the behavior of the decision variables of the power plant on its optima. Such approach results in a novel mathematical formulation shaped as a system of non-linear equations and additional constraints that is able to easily provide accurate estimations of the optimal values of the power plant design and operative variables.

Keywords: *thermodynamic optimization; economic optimization; combined cycle power plants; optimal relationships*

Nomenclature:

Mathematical Symbols

f_e = economic objective function

f_e^* = economic objective function – optimal value

$\hat{f}_e$ = economic objective function – estimated value

f_t = technical objective function

f_t^* = technical objective function – optimal value

$\hat{f}_t$ = technical objective function – estimated value

h = set of equality constraints

g = set of inequality constraints

$\underline{x}$ = model variables

$\underline{x}^*$ = model variables – optimal values

$\underline{\hat{x}}$ = model variables – estimated values

$\underline{x}_k$ = model variables – decision variables

$\underline{R}_j$ = Ratio

$\underline{R}_j^*$ = Ratio – optimal values

$\underline{\hat{R}}_j$ = Ratio – estimated values

r_d = design ratio

ψ = functional relationships

α = tolerance parameters for the functional relationships

γ = adjustment parameters for the functional relationships

φ = economic optimal relationships

β = tolerance parameters for the economic optimal relationships

δ = adjustment parameters for the economic optimal relationships

Abbreviations

$HRSG$ = heat recovery steam generator

$CCGT1P$ = 1 pressure level combined cycle gas turbine power plant

$CCGT3P$ = 3 pressure levels combined cycle gas turbine power plant

Power Plant Model Variables

η_T = thermal efficiency

η_E = exergetic efficiency

A_{Net} = net heat transfer area

A_e = specific transfer area

$\dot{W}_{Net}$ = net power production

W_0 = power demand

$\dot{Q}_{Net}$ = net energy consumption

$\dot{E}_{Net}$ = net exergy destruction

Economic Variables

RC_u = unit costs ratio

a = transfer area cost factor

CRF = capital recovery factor

POT = annual plant operative time

CW_u = unit cost of turbines

CA_u = unit cost of transfer area

CF_u = unit cost of fuel

TAC = total annual cost

TAC_e = specific annual cost

1. Introduction

1.1. Power Plant Optimization based on Economic Criteria

The optima characteristics identified based on thermodynamic optimization can be made more realistic through subsequent refinements accomplished by benefits maximization or costs minimization. It is beyond dispute that in the end any practical engineering design will be selected only as it yields unmatchable values of its financial indicators. Biezma and San Cristóbal [1] and Remer and Nieto [2, 3] described uses and limitations of many different project evaluation techniques and showed how they may be applied to cogeneration plants.

In the industrial practice, design and operation of power plants usually bring up two types of optimization opportunities. First, for an existing facility, repowering the system is important for maintaining the profits margin when facing increases of fuel price and other operative costs. On the other hand, when designing a new power plant, it becomes critical to select the appropriate equipment and to determine the operative parameters that guarantee the required power demand can be satisfied and that good values of the project financial indicators will be achieved.

Kotowicz and Bartela [4] studied the influence of fuel price variations on the steam part of a combined cycle power plant, by means of a genetic algorithm based optimization programme. Increasing fuel prices have a noticeable impact on the optimal values of the decision variables, and ultimately, cause unavoidable increments on the operative costs. They also observed that thermodynamic and economic optima for a given fuel price, within the studied range of prices, differ from each other in a quite small percentage over the final cost of the generated energy.

Poma et al. [5] improved the initial design of a waste-to-energy plant integrated with a combined cycle through a thermoeconomic procedure, and accomplished a reduction in the unit cost of electricity and an increment on the power production. In addition, different alternatives were economically evaluated using thermodynamic optimal values of the plant variables (but not economic optimal ones), which allowed selecting good configurations for each market condition scenario.

Mussati et al. [6] presented a hybrid methodology which is able to provide lower and upper bounds on the economic optimal solution of combined heat and power plants and desalination systems, by using relationships between the thermodynamic and economic optima. Even tough, the economic optimal design of a complex energy system usually turns out to be quite challenging, due to the large number of decision variables involved and the inherently non-linear nature of the problem.

Other authors have elaborated more complex strategies in an attempt to find a compromise between economic and thermodynamic analysis of diverse processes. In this context, exergy-based economic analysis methodologies are based on the proposition that the role of energy should be defined and understood through the second law of thermodynamics in terms of the costs and benefits of utilizing exergy (i.e. available energy) to accomplish a specified work.

Franco and Casarosa [7] showed how the thermal efficiency can rise over the actual limit of 60% for combined plants designed at its thermoeconomic optima, based on the minimization of the total cost of the plant per unit power, obtained referring to a common economic basis the cost of the exergy losses and the costs of the components. Valdés et al. [8] presented a thermoeconomic optimization model regarding the HRSG of a combined cycle plant, and as result showed that it is possible to find an optimum for every selected design parameter, although such optimum depends on the selected optimization strategy.

Rosen and Dincer [9] stated that a systematic correlation appears to exist between exergy loss rate and capital cost for coal-fired, oil-fired and nuclear generating stations (and that this idea may extend to other technologies), which imply that its components are configured to achieve an overall optimal design, by appropriately balancing the exergy-based thermodynamic and the economic characteristics of the system.

1.2. Synthesis and Design of Power Plants Aiming at their Thermodynamic Optimization

Synthesis and design of power generation systems is performed in first instance aiming at improving the system technical performance. Then, thermodynamic optimization improves energy efficiency and saving, by identifying ways to better utilize the available resources. Several strategies have been proposed in the literature for increasing the thermodynamic effectiveness of power plants, starting with the simpler maximization of the system thermal efficiency; while on the other end, elaborated approaches have been suggested in order to include in the analysis a more detailed insight of the system characteristics.

Franco and Giannini [10] defined a decomposition strategy by organizing the optimization of the power plant into two levels; enabling the first one to obtain the main operative parameters by minimizing exergy losses; and acquiring a detailed design of the HRSG sections in the second level by optimizing different geometrical parameters.

Valdéz and Rapún [11] presented a method for the optimization of a HRSG based on the utilization of influence coefficients, which takes advantage of the influence of the design parameters on the cycle thermodynamic performance; although its application to multiple pressure configurations becomes complex due to the need of evaluating a big number of combinations.

Bassily [12], using a three pressure level combined cycle as case study, compared the results obtained from thermodynamic optimization relative to the operative parameters, a method they proposed for irreversibility reduction of the HRSG, and a typical commercially available plant. As result, they observed that the optimized cycle reaches a thermal efficiency 1.7% higher than the reduced-irreversibility cycle, and 3.6-3.8% higher than the regularly designed cycle.

Woudstra et al. [13] explored the potential for improvement of a power cycle by using the so-called internal exergy efficiency, which intends to measure the difference between the actual exergy losses with the ones of the corresponding ideal reversible case. By using such performance indicator, they pointed out which of the power plant components are more susceptible to design and operative enhancements.

Scenna and Aguirre [14] stated that sets of thermodynamic heuristics derived from the universal thermodynamic properties can be used to facilitate the optimization of the system under consideration, as they can be used to efficiently construct operative profiles for the system operative characteristics. Moreover, they presented heuristics regarding electricity generation cycles that proved to be useful during the initialization phase of the optimization procedure of such systems.

Other authors have focused their research from a more theoretical approach, although their results are able to provide more general rules regarding the thermodynamic optimal behavior of diverse systems and how to design such systems while accomplishing improvements from the second law point of view. Tondeur and Kvaalen [15] stated that in a contacting or separation device with a given transfer area and a specified duty, the total entropy produced is minimal when the local rate of entropy production is uniformly distributed, or equipartitioned, along the space and/or time variables. Later, Nummedal and Kjelstrup [16] proposed that a family of operating lines named isoforce operating lines (i.e. relations between constant driving forces and the corresponding minimum entropy production rates) may be used to assess the efficiency of heat exchangers, and accomplish area reductions by replacing normal operation by isoforce operation.

Vargas and Bejan [17] studied the thermodynamic behavior of a power plant associated solely with the stream-to-stream interaction while operating at maximum power, and demonstrated that thermodynamic optima exist with respect to both the mass flow ratio and the area allocation ratio for this simple system; and they also mentioned that it may be useful to extend these relationships to more complex systems. By following their ideas, Godoy et al. [18] found families of optimal thermodynamic solutions for a one pressure level combined cycle gas turbine power plant, which summarize trends of the optimal exergetic efficiency and the associated optimal values of design and operative variables. Then, these families let knowing in advance optimal values of the decision variables when facing changes of power demand or adjusting the design to an available heat transfer area.

1.3. Aim and Outline of this Work

In this context and aiming at simplifying the optimization procedure, a new strategy which allows accurately estimating the economic optimal characteristics of the studied combined cycle power plants including the associated optimal values of its main design and operative variables is presented, when the following instances here explored are considered:

- The economic optima of power plants (for minimum values of the specific annual cost) present distinctive characteristics for wide ranges of market conditions (as given by the relative weights of capital investment and operative costs).
- Relationships between the economics and thermodynamics of the here considered power plant configurations exist, that relate the economic optima characteristics with the optimal solutions of thermodynamic optimization formulations.

Such strategy takes advantage of previous results presented by the authors (Godoy et al. [18]), and an adequate manipulation of functional relationships among the thermodynamic optimal values of the decision variables. When systematically applying these obtained functional relationships, the reduction of the feasible region (defined by the optimization problem constraints) is accomplished, and at the end, the resolution procedure of the optimization problem becomes equivalent to solving the resultant set of non-linear equations system and additional constraints so achieved to optimize the power plant characteristics.

2. Non-Linear Programming Model of the Combined Cycle Gas Turbine Power Plants

2.1. Power Plants Configuration

Two different gas turbine combined cycle power plants are used as case study, which are next briefly described. Simplified flow diagrams of each power plant are also presented.

CCGT1P, A Small Scale Power Plant: A combined cycle which consists of a gas turbine, its associated one pressure level HRSG, and a steam turbine, is used as small scale power plant case study (a similar system is analyzed in Godoy et al. [18], although with some configuration differences respect to the one here used). A schematic description is presented in Figure 1.

CCGT3P: A Large Scale Power Plant: a combined cycle which consists of two gas turbines with postcombustion and regeneration, its associated three pressure level HRSGs, and a steam turbine with high, intermediate and low pressure stages, is used as large scale power plant case study (see Bassily [3], Franco and Casarosa [19]). A schematic description is presented in Figure 2. Using this innovative cycle enables to obtain high efficiencies, as the following features are taken into account:

- Gas to gas recuperation in the gas cycle
- Postcombustion between the two stages of the gas turbine
- High gas turbine inlet temperature (up to 1500 K)
- Multiple pressure levels in the HRSG
- Parallel heat exchange sections in the HRSG

2.2. Power Plants Model

The mathematical model of the power plant is implemented through a series of modules, which in conjunction describe the design and operative characteristics of such systems (for a more detailed description of the power plant model refer to Appendix A) and that allows representing any of the combined cycles used as case study.

In order to test this model, CCGT1P and CCGT3P results here obtained are compared to the design and operative parameters of a small scale power plant, MS9001FA 1x1 from GE Power

Systems (GE [20]), and a large scale power plant, SCC5-4000F 2x1 from Siemens (Siemmens [21]), respectively. The resultant mathematical problem is solved by means of the software GAMS (Rosenthal [22]) running in “simulation mode” (i.e. using a variable which has no influence on the rest of the power plant model as objective function), by means of the reduced gradient algorithm CONOPT (Drud [23]).

Table 1 and Table 2 list the values of the main practical interest variables obtained with the CCGT1P and CGT3P model, respectively, paired with the ones associated to the commercial power plants. It should be noted that similar values of the operative conditions are obtained with the here proposed model respect to the commercial power plants, although for designs based on larger power production capacities. Nevertheless, reported operative conditions fall within the usual ones for actual power plants. In addition, good values of the computational requirements (iteration count and resolution time) are obtained.

From Table 2, it can be seen that CCGT3P model reaches a higher thermal efficiency than the commercial power plant used as reference. Such result can be explained through the innovative features considered in CCGT3P model, including configuration improvements and operative conditions enhancements (see Appendix A).

3. Useful Thermodynamic Relationships among Decision Variables

3.1. Optimizing the Power Plants using the Thermodynamic Efficiency as Technical Performance Indicator

Thermodynamic optima of a power plant are usually obtained as its first law efficiency or second law efficiency is maximized. The thermal efficiency of the power plant (i.e. net power production per unit of energy supplied as fuel, as given by Eq. (1)) is usually used as first law efficiency (see for example Valdés and Rapún [11]).

$$\eta_T = \frac{\dot{W}_{Net}}{\dot{Q}_{Net}} \tag{1}$$

Even though, the irreversible losses of the system are not quantified by the first law efficiency since it makes no distinction between power and heat. Regulagadda et al. [24] conducted energy and exergy parametric studies of a coal-fired power plant. For different operative conditions, they showed that behavior of energy and exergy efficiencies follow similar trends; although, exergy efficiency values are always lower than the corresponding energy efficiency ones. Analogous results in comparing efficiencies results were presented by the authors (see Godoy et al. [18]).

Taking into account conclusions obtained by Godoy et al. [18] and Regulagadda et al. [24] and considering that the thermal efficiency is widely used in the industrial practice to measure power plants technical performance, that definition of the CCGT efficiency will be used here as the thermodynamic objective function. Then, an extended approach of the thermodynamic optimization is presented to identify trends on the power plant optimal behavior as parametric analysis of the decision variables is performed within a practical application range.

As power production and total heat transfer area constitute two of the most important attributes to be considered when designing or repowering a power generating facility, their joint influence in the thermodynamic optima can be gathered by means of the specific heat transfer area, as defined by Eq. (2).

$$A_e = \frac{A_{Net}}{\dot{W}_{Net}} \tag{2}$$

The mathematical statement of the thermodynamic optimization problem, hereafter named Problem P1, is given by Eqs. (3-6). Here, the thermal efficiency $\eta_T(\underline{x}, A_e)$ is maximized in order to obtain optimal values of all the power plant model variables $\underline{x}$ linked to its design and operation, subject to all the equality and inequality constraints ($h(\underline{x}, r_d)$ and $g(\underline{x}, r_d)$, respectively) included in the base model of the power plant (and further described in Appendix A), for different values of the specific heat transfer area A_e. Also, an upper bound on the power production is imposed.

Problem P1:

$$\max \eta_T(\underline{x}, A_e) \tag{3}$$

$$h(\underline{x}, A_e) = 0 \tag{4}$$

$$g(\underline{x}, A_e) \leq 0 \tag{5}$$

$$\dot{W}_{Net} \leq W_0 \tag{6}$$

$$\underline{x} \in \Re^n$$

The generated problem is implemented in the optimization software GAMS (Rosenthal [22]), and is solved using the reduced gradient algorithm CONOPT (Drud [23]). Resolution of the NLP optimization problem is performed for wide ranges of specific transfer area values, from 170

m^2/MW to 760 m^2/MW for CCGT1P, and from 360 m^2/MW to 1000 m^2/MW for CCGT3P.

After achieving thermodynamic optimal values of the power plant characteristics, optimal values of selected decision variables $\underline{x}_k^*$ can be re-expressed as function of the specific transfer area A_e, as stated by Eq. (7).

$$\underline{x}_k^* = \underline{x}_k^*(A_e) \ \ , \ \ \underline{x}_k^* \subset \underline{x}^* \tag{7}$$

Evolution of the optimal thermal efficiency against the specific transfer area reflects that the optimal thermal efficiency exhibits an increasing trend, up to a value of the specific transfer area of 260 m^2/MW for CCGT1P and 480 m^2/MW for CCGT3P, as presented in Figure 3. Further increments of the specific transfer area are not reflected on the maximum value of the thermal efficiency, as it remains unaltered; therefore, these segments of the efficiency vs. area curves are not graphically presented. Similarly, Godoy et al. [18] found that the optimal exergetic efficiency of a one pressure level CCGT power plant increases as the power to area ratio does, up to a given value of the specific transfer area.

Then, thermodynamics set an upper bound on the total transfer area to be assigned to a given power generating facility (up to 260 m^2/MW for CCGT1P and 480 m^2/MW for CCGT3P), which will enable improvements on its operation and design from such point of view. For example, when observing CCGT1P for a desired net power production, the cut value of the specific transfer area indicates when it is desirable to shift from a 1 pressure level design to a configuration with more operative pressures levels, as assigning additional area to CCGT1P has no positive effect on its thermodynamic performance.

It should be noted that these cut values of the specific transfer area depends upon the characteristics of the power plant, and even on the hypothesis adopted on its mathematical model, although the observed trends are still discerned in spite of this considerations. For instance, Godoy et al. [18] showed there is a maximum attainable thermodynamic efficiency for a one pressure level CCGT power plant with some configuration and operative differences respect to the one used here as case study when its design is based on a specific transfer area of around 237 m^2/MW.

Associated to the optimal thermal efficiency values presented in Figure 3, optimal values for the design and operative variables of the CCGT power plants are also systematically attained. Then, for a given value of the specific transfer area, it is possible to identify optimal values of the transfer areas of the HRSG sections, the power production of each turbine, the fuel consumption, the operative pressures, the steam flow rate for each operative pressure level, and so on.

From an operative and design point of view, these thermodynamic optimal solutions represent in advance optimal CCGT power plants that are obtained when facing changes of the power demand or adjusting the design to an available heat transfer area.

3.2. Finding Optimal Thermodynamic Functional Relationships

According to previous results (see Godoy et al. [18]), it is possible to find practical Ratios among the decision variables of the power plant, which behave smoother when the thermodynamic optima is surveyed in search of functional relationships. Here, such Ratios definitions are extended to the more complex CCGT3P power plant, covering power production distribution, transfer area allocation, compression and expansion ratios, HRSG operative temperatures relations, specific fuel consumption and air and steam flow rates relations, as defined in Eq. (8) and listed in Table 3.

$$\underline{R}_j = f\left(\underline{x}_k\right) \tag{8}$$

As Godoy et al. [18] showed for a similar power plant configuration characterized by maximum values of its exergetic efficiency, all functional relationships associated to a one pressure level combined cycle are inherently linear. When optimizing the thermal efficiency, it is observed that the proposed Ratios for CCGT1P also exhibit a linear behavior respect to the specific transfer area within the range from 170 m^2/MW to 260 m^2/MW. Moreover, functional relationships for most of the proposed ratios associated to CCGT3P can be assumed as linear with no precision losses, for values of the specific transfer areas within the range from 360 m^2/MW to 480 m^2/MW. Such specific transfer area ranges represent those design and operative scenarios where the optimal thermal efficiency for each case study is influenced by the specific transfer area value (see Section 3.1), and therefore, correspond to practical interest situations as performance improvements may be achieved.

Based on these ideas, an easy to implement procedure to provide accurate estimations of the optimal values of the decision variables, within the whole design and operative ranges broaden for the here considered case studies, is introduced.

In our case and linked to the optimal solutions of the thermodynamic optimization formulation (Problem P1), a NLP mathematical model, hereafter named Problem P2, is formulated as given by Eqs. (9-14), in order to search for functional relationships regarding the decision variables of the power plant when the specific transfer area is selected as interest design ratio. Tolerance parameters $\alpha_j(A_e)$ are minimized, which allows finding functional relationships $\psi_j\left(\underline{\hat{R}}_j, A_e, \gamma_{lj}\right)$ that accurately predict the thermodynamic optimal values of the practical interest Ratios for wide ranges of values of the specific transfer area A_e.

Problem P2:

$$\min \sum_j \sum_{A_e} \alpha_j(A_e) \tag{9}$$

$$h\left(\underline{\hat{x}}, A_e\right) = 0 \tag{10}$$

$$g\left(\underline{\hat{x}}, A_e\right) \leq 0 \tag{11}$$

$$\dot{W}_{Net} \leq W_0 \tag{12}$$

$$\hat{\eta}_T\left(\underline{\hat{x}}, A_e\right) \leq \eta_T^*\left(\underline{x}^*, A_e\right) \tag{13}$$

$$\left[\psi_j\left(\underline{\hat{R}}_{\mathrm{j}}, A_e, \gamma_{lj}\right) - \underline{R}_j^*(A_e)\right]^2 \leq \alpha_j(A_e) \tag{14}$$

$$\underline{\hat{x}} \in \Re^n \quad , \quad \alpha_j \geq 0$$

Within this NLP problem, the sets of equality and inequality constraints (given by Eqs. (10-11), respectively) remain the same as in the original optimization problem (Problem P1). Meanwhile, the optimal values of the technical objective function $\eta_t^*\left(\underline{x}^*, A_e\right)$ found when solving the original optimization problem are set as upper bounds on the values of such function $\hat{\eta}_t\left(\underline{\hat{x}}, A_e\right)$ which is now computed for the estimated values of the decision variables $\underline{\hat{x}}_k$, according to Eq. (13). The generated problem is implemented in the optimization software GAMS (Rosenthal [22]), and is solved using the reduced gradient algorithm CONOPT (Drud [23]).

As mentioned above, if linear functionality is assumed, the mathematical expression given in Eq. (15) can be used to correlate each Ratio as function of the specific transfer area. In addition, using a linear expression presents the advantage that adjustment of the functional relationships may be accomplished with thermodynamic optimal solutions for only two different values of the specific transfer area within the practical application range. This method for obtaining the adjustment parameters is less computationally expensive as it requires not solving the thermodynamic optimization problem more than twice.

$$\underline{\hat{R}}_j = \gamma_{1j} A_e + \gamma_{2j} \quad (15)$$

The values of the adjustment parameters γ_{1j}, γ_{2j} for Ratios associated to CCGT1P and CCGT3P are listed in Table 4 and Table 5, respectively. Moreover, a brief description of the evolution of the studied Ratios associated to CCGT1P and CCGT3P decision variables is presented in Appendix B.

Evolution of the design and operative variables for practical ranges of the specific transfer area is exemplified in Figure 4, by plotting the optimal values of the HRSG area allocation ratio AAR_{HRSG} for CCGT3P. In addition, the corresponding linear functional relationship is plotted, in order to show the application of the proposed procedure. For this example, the corresponding linear functional relationship is able to predict the optimal value of the HRSG area allocation ratio with an accuracy level of 99.35%.

Nevertheless, in order to portray the slightly non-linear behavior that some of the functional relationships (in particular those associated to CCGT3P) exhibit, a more general coverage for the thermodynamic optima correlation is required. So, a more general mathematical expression (for example, a second order polynomial) can be used to correlate each Ratio as function of the specific transfer area.

Several research works presented by other authors (as for example [14], [17]) have been devoted to the idea of using heuristics derived from the universal thermodynamic properties to obtain profiles for the system operative characteristics respect to the parameters that govern the behavior of the studied system. The here proposed functional relationships constitute a systematic approach to these notions, as they efficiently summarize the thermodynamic optima attributes.

Then, once all the adjustment parameters γ_{1j}, γ_{2j} have been determined for all the proposed Ratios, Eq. (15) can be used to compute accurate estimations of the optimal values of the decision variables, within the whole ranges of values of specific transfer areas broaden for the here considered case studies.

4. Economic Optimization of the Power Plant

In this work, the specific annual cost of the power plant (i.e. the total annual cost per unit of generated power) is selected as economic indicator (see Biezma and San Cristóbal [1], Remer and Nieto [2, 3]), as given by Eq. (16). The main investment and operative costs are considered for computing the specific annual cost of the facility, including acquisition costs of turbines, and operative costs due to fuel consumption.

$$TAC_e = \frac{TAC}{\dot{W}_{Net}} = (CW_u.CRF) + (CA_u.CRF).\frac{(A_{Net})^a}{\dot{W}_{Net}} + (CF_u.POT).\frac{\dot{m}_F}{\dot{W}_{Net}} \quad (16)$$

Then, the obtained economic optima and the associated values of the decision variables strongly depend on the values of the unit investment and operative costs. Here, the relative weight of the unit costs of fuel and area on the economic optima is studied by means of the costs ratio, as defined by Eq. (17). Such ratio is varied across a wide range, which allows observing the behavior of the economic optima when the fuel unit cost overshadows the area unit cost, and vice versa.

$$RC_u = \frac{CF_u'.POT}{CA_u'.CRF} \quad (17)$$

So, the mathematical statement of the economic optimization problem, hereafter named Problem P3, gets as given by Eqs. (18-21). Here, the specific annual cost of the facility $TAC_e(\underline{x}, RC_u)$ is minimized in order to obtain optimal values of all the power plant model variables $\underline{x}$ linked to its design and operation, subject to all the equality and inequality constraints ($h(\underline{x}, p)$ and $g(\underline{x}, p)$, respectively) included in the base model of the power plant (and further described in Appendix A), for different values of the costs ratio RC_u. Also, a lower bound on the power production is imposed.

Problem P3:

$$\min TAC_e(\underline{x}, RC_u) \quad (18)$$

$$h(\underline{x}, RC_u) = 0 \quad (19)$$

$$g(\underline{x}, RC_u) \leq 0 \quad (20)$$

$$\dot{W}_{Net} \geq W_0 \quad (21)$$

$$\underline{x} \in \Re^n$$

The generated problem is implemented in the optimization software GAMS (Rosenthal [22]), and is solved using the reduced gradient algorithm CONOPT (Drud [23]). As result of solving the optimization problem, a family of optimal values of the objective function $TAC_e^*(\underline{x}^*, RC_u)$ are obtained, associated to given values of the costs ratio RC_u. Then, resulting optimal values of selected decision variables $\underline{x}_k^*$ can be re-expressed as function of the costs ratio RC_u, as stated by Eq. (22).

$$\underline{x}_k^* = \underline{x}_k^*(RC_u) \quad , \quad \underline{x}_k^* \subset \underline{x}^* \tag{22}$$

Resolution of the NLP optimization problem is performed for a wide range of values of the costs ratio, for both CCGT power plants used here as case studies. Evolution of the optimal specific annual cost against the costs ratio is presented in Figure 5 for CCGT1P and CCGT3P. Note that in this figure, only a reduced range is presented, where change of the objective function is more significant and including the practical scenarios for the actual market conditions; nevertheless, the here presented analysis can be extended to far lower and higher costs ratio values.

Figure 5 shows that the optimal specific annual cost rapidly diminishes as the costs ratio increases. For costs ratio values higher than 0.05, it can be seen that the optimal specific annual cost becomes asymptotic to a value of 0.083 M$/MW for CCGT1P and 0.072 M$/MW for CCGT3P. On the other end, as the costs ratio diminishes, the optimal value of the specific annual cost increases following an exponential trend.

The costs distribution on the economic optima is presented in Figure 6 and Figure 7 for CCGT1P and CCGT3P, respectively. In both case studies, for costs ratio values lower than (approximately) 0.001, the investment cost on transfer area dominates the economics of the power plant, as it can represent up to 95% of the specific annual cost.

In opposition, for costs ratio values higher than (approximately) 0.001, it can be seen in Figure 6 and Figure 7 that the operative costs due to fuel consumption have a larger impact on the power plant economics than the investment costs (associated here to turbines and HRSGs costs). Then, when designing and operating in this range of values of the costs ratio, efforts dedicated to increasing the power generation efficiency are indispensible, even more in a market as the actual one where the fuel price exhibits an increasing trend. Kotowicz and Bartela [4] studied the susceptibility of a selected economic objective function with respect to changes of the price of supplied gas and the capital costs, by varying both quantities 20% in relation to their nominal values. For actual market conditions, they also found that the largest influence on the plant economics is exerted by changes of the costs of fuel.

It should be noted that the reported results depend on the adopted values of the economic factors. For example, the exponent used for the calculation of the acquisition cost of the HRSG is here fixed at 0.6, although other values, always below 1, can be found in the literature. Another example is the capital recovery factor, which is here computed for a given value of the interest rate. Then, influence of such factors on the economic optima can be studied by means of a complete sensitivity analysis; although such study exceeds the extent of this work.

As previously pointed out, associated to the sets of optimal specific annual cost values presented in Figure 5, sets of optimal values for the design and operative variables of the CCGT power plants are also systematically attained. Then, for a given value of the costs ratio, it is possible to identify optimal values of the transfer areas of the HRSG sections, the power production of each turbine, the fuel consumption, the operative pressures, the steam flow rate for each operative pressure level, and so on.

4.1. Relationship between the Economic and Thermodynamic Optima of the Power Plants

For the here considered case studies, relationship between the economic and thermodynamic optima of the power plants is explored by surveying the thermodynamic and economic optima characteristics. The aim of this analysis is to distinguish if, and when, the optimal thermodynamic solutions also represent economic optima of the CCGT power plants for given market conditions.

Thermodynamic optima of CCGT1P and CCGT3P are previously determined by means of Problem P1, as the thermal efficiency is maximized for wide ranges of the specific transfer area. Moreover, optimal values of the decision variables, including design and operative ones, were determined for each given value of the specific transfer area. Then, for a given value of the specific transfer area, optimal values of the transfer areas of the HRSG sections, the power production of each turbine, the fuel consumption, the operative pressures, the steam flow rate for each operative pressure level, etc., can be identified.

At this time, by means of Eq. (16), it becomes possible to compute the specific annual cost values associated to the thermodynamic optima of CCGT1P and CCGT3P, for wide ranges of values of the costs ratio. The calculated values of the specific annual cost are presented in Figure 8 and Figure 9 for CCGT1P and CCGT3P, respectively. It can be noticed that the specific annual costs associated to the thermodynamic optima are highly dependent on the costs ratio value, while only slight variations against the specific transfer area are observed.

In addition, in Figure 8 and Figure 9, the optimal values of the specific annual cost of CCGT1P and CCGT3P (obtained by economic optimization with Problem P3) are also plotted, by utilizing the costs ratio values as parameter, and the economic optimal values of the specific transfer area associated to each given value of the costs ratio.

By analyzing Figure 8 and Figure 9, it can be deduced that an optimal value of the specific transfer area exists for each value of the costs ratio where the thermodynamic optima and the economic optima are equivalent, i.e. where the specific annual costs associated to the thermodynamic optima equal the optimal values of the specific annual cost obtained by economic optimization. In other words, the economic optima are supported on the feasible space of thermodynamic optimal solutions; and relation between both optima is determined by a given value of the specific transfer area for each given value of the costs ratio.

In order to find the sets of values of specific transfer area that link the thermodynamic and economic optima, the optimal values of the specific transfer area found by means of economic optimization for each given value of the costs ratio are used as parameters for solving a thermodynamic oriented optimization of the power plants.

The mathematical statement of the resultant modified thermodynamic optimization formulation, hereafter named Problem P4, is based on Problem P1. The thermal efficiency $\eta_T\left(\underline{x}, A_e|_{Economic}\right)$ is maximized, subject to all the equality and inequality constraints included in the base model of the power plant (and further described in Appendix A). In addition, this modified thermodynamic optimization problem is solved for the optimal value of the specific heat transfer area $A_e|_{Economic}$ associated to each given value of the costs ratio used as parameter for solving the economic optimization problem (i.e. Problem P3). In other words, now the economic optimal values of the specific transfer area $A_e|_{Economic}$ related to each given value of the costs ratio are set as parameters for obtaining optimal solutions of the thermodynamic optimization problem.

As result of solving the modified thermodynamic optimization problem (i.e. Problem P4), maximum values of the thermal efficiency, as well as optimal values of the design and operative variables of the power plant, are obtained for each value of the specific transfer area associated to a given value of the costs ratio. By using such optimal variables, it becomes possible to calculate the specific annual cost values associated to the thermodynamic optima of CCGT1P and CCGT3P, by means of Eq. (16).

Then, it can be noticed that costs values so computed present the same values than the optimal ones obtained by means of economic optimization for the corresponding value of the costs ratio. In addition, not only the optimal values of the specific annual cost are identical, but also the optimal values of the design and operative variables of the power plants. In other words, it can be concluded that both achieved solutions are equivalent for the condition previously specified.

Then, it is clear that the optimal solution of the modified thermodynamic optimization problem (i.e. the thermodynamic optima for the economic optimal value of the specific transfer area corresponding to a given costs ratio, obtained by means of Problem P4) is equivalent to the optimal solution of the corresponding economic optimization problem (i.e. the economic optima for the same given value of the costs ratio, obtained according to Problem P3).

When the specific transfer area is fixed, all the capital costs included in the specific annual cost (which is here selected as economic objective function) get also fixed, and the aim of the economic optimization becomes minimizing the operative costs due to fuel consumption. Such target is the same of a thermodynamic optimization where the thermal efficiency is selected as technical performance indicator, and generates the previously revealed equivalence between the economic optima and the optimal solution of the modified thermodynamic optimization problem.

4.2. Economic Optimal Relationship for the Specific Transfer Area against the Costs Ratio

Linked to the optimal solutions of the economic optimization formulation (i.e. Problem P3), a NLP mathematical model, hereafter named Problem P5, is introduced to search for an economic optimal relationship between the economic optimal values of the specific transfer area and the costs ratio (which is selected as interest parameter), as given by Eqs. (23-28). Tolerance parameters $\beta_{A_e}(RC_u)$ are minimized, which allows finding the economic optimal relationship $\varphi_{A_e}(\hat{A}_e, RC_u, \delta_{lA_e})$ by means of Eq. (28), that accurately predicts the economic optimal values of the specific transfer area for the studied range of values of the costs ratio RC_u.

Problem P5:

$$\min \sum_{RC_u} \beta_{A_e}(RC_u) \quad (23)$$

$$h\left(\underline{\hat{x}}, RC_u\right) = 0 \quad (24)$$

$$g\left(\underline{\hat{x}}, RC_u\right) \leq 0 \quad (25)$$

$$\dot{W}_{Net} \geq W_0 \quad (26)$$

$$T\hat{A}C_e\left(\underline{\hat{x}}, RC_u\right) \geq TAC_e^*\left(\underline{x}^*, RC_u\right) \quad (27)$$

$$\left[\varphi_{A_e}\left(\hat{A}_e, RC_u, \delta_{lA_e}\right) - A_e^*(RC_u)\right]^2 \leq \beta_{A_e}(RC_u) \quad (28)$$

$$\underline{\hat{x}} \in \Re^n \quad , \quad \beta_{A_e} \geq 0$$

Within this NLP problem, the sets of equality and inequality constraints (given by Eqs. (24-25), respectively) remain the same as in the original optimization problem (Problem P3), as well as the lower bond imposed on the power production (given by Eq. (26)). Meanwhile, the optimal values of the objective function $TAC_e^*\left(\underline{x}^*, RC_u\right)$ found when solving the original optimization problem are set as lower bounds on the values of such function $T\hat{A}C_e\left(\underline{\hat{x}}, RC_u\right)$ which is now computed for the estimated values of the decision variables $\underline{\hat{x}}_k$, according to Eq. (27). The generated problem is implemented in the optimization software GAMS (Rosenthal [22]), and is solved using the reduced gradient algorithm CONOPT (Drud [23]).

Economic optimal values of the specific transfer area versus the costs ratio (obtained according to Problem P3) are plotted in Figure 10 and Figure 11 for CCGT1P and CCGT3P, respectively. For CCGT1P, the specific transfer area becomes invariable for values of the costs ratio below approximately 0.00086 and above approximately 0.17 (see Figure 10), at constant values of 124.6 m^2/MW and 254.2 m^2/MW, respectively. For CCGT3P, the specific transfer area becomes invariable for values of the costs ratio below approximately 0.00034 and above approximately 0.43 (see Figure 11), at constant values of 308.1 m^2/MW and 478.5 m^2/MW, respectively.

Note that these values are associated to the economic optimal solutions follow a sigmoid behavior. Then, a sigmoid function, given by the general function presented in Eq. (29), is selected to correlate the specific transfer area as a function of the costs ratio, covering this way the whole ranges of values of the costs ratio with a single functionality.

$$\hat{A}_e = \frac{\delta_{1A_e}}{1 + exp\left(\delta_{2A_e} RC_u + \delta_{3A_e}\right)} \quad (29)$$

The mean errors introduced by Eq. (29) on the estimation of the economic optimal values of the specific transfer area for the studied ranges of values of the costs ratio are 0.30% for

CCGT1P and 0.18% for CCGT3P. The corresponding values of the adjustment parameters $\delta_{1A_e}, \delta_{2A_e}, \delta_{3A_e}$ for the here studied power plant configurations are presented in Table 9. Graphical representations of the values of the specific transfer area estimated by Eq. (29) according to the values of the adjustment parameters listed in Table 9 are presented in Figure 10 and Figure 11 for CCGT1P and CCGT3P, respectively.

Therefore, once all the adjustment parameters $\delta_{1A_e}, \delta_{2A_e}, \delta_{3A_e}$ have been determined, Eq. (29) can be used to compute accurate estimations of the economic optimal values of the specific transfer area, within the whole ranges of values of the costs ratio broaden for the here considered case studies.

Nevertheless, if the range of costs ratio values is narrowed around the actual market conditions, a linear expression may be used to compute the economic optimal value of the specific transfer area for a given value of the costs ratio with a negligible value of the estimation error.

5. A Simplified Approach for Addressing the Economic Optimization of Power Plants, by means of a Non-Linear Equations System plus Additional Constraints

Efforts are here oriented towards finding ways for accurately estimating economic optimal solutions for the power plant model without having to solve the corresponding mathematical optimization problem. To accomplish this aim, the following previously explored premises are considered:

- the optimal solution of a thermodynamic optimization problem where the specific transfer area is fixed at the economic optimal value for a given costs ratio is equivalent to the optimal solution of the corresponding economic optimization problem for the same given value of the costs ratio (see Section 4.1)
- the economic optimal relationship for the specific transfer area is able to provide accurate estimations of the economic optimal values of the specific transfer area for a given value of the costs ratio (see Section 4.2)

Then, it becomes possible to implement a strategy aiming at simplifying the resolution of the economic optimization problem of power plants. In fact, it is possible to take advantage of the relationships between the thermodynamic and the economic optima of the power plants, as the economic optimal relationship can be introduced in order to fix the specific transfer area in the economic optimal value for a given costs ratio. Then, the functional relationships that summarize the thermodynamic optima characteristics can be used as new constraints into the economic optimization problem, as it was previously shown that they also contain the economic optima information.

This strategy presents a large independence of the economic parameters (as it is only necessary to provide economic optima information about the economic optimal value of the specific transfer area), and takes advantage of the wider space of feasibility of the thermodynamic optima of the power plants. Therefore, in this section, this “thermodynamic” approach will be further explored.

As one or more functional relationships are introduced in the original optimization problem, the reduction of the space of thermodynamic feasible solutions is accomplished. Once the economic optimal relationship for the specific transfer area plus enough functional relationships are introduced in the original economic optimization problem (i.e. Problem P3) in order to fix all its degrees of freedom, resolution of this modified mathematical problem becomes equivalent to solving the resultant system of non-linear equations and additional constraints, which delivers a unique (estimation of the optimal) solution for a given value of the costs ratio. This procedure simplifies the resolution of the optimization problem and reduces the associated computational requirements.

The formulation of the resulting system of non-linear equations and additional constraints, hereafter named Problem P6, is composed by the following sets of equations:

- the economic optimal relationship which accurately predicts the economic optimal value of the specific transfer area for a given value of the costs ratio, reproduced in Eq. (30)
- the functional relationships found for the thermodynamic optima, which allow accurately estimating the optimal values of the decision variables for given values of the specific transfer area, given by the set of constraints reproduced in Eq. (31)
- the power production requirement, fixed according to Eq. (32)
- the equality and inequality constraints defined according to the power plant model, as given by Eqs. (33-34)

$$\hat{A}_e = \frac{\delta_{1A_e}}{1+exp(\delta_{2A_e}RC_u+\delta_{3A_e})} \quad (30)$$

$$\underline{\hat{R}}_j = \gamma_{1j}\hat{A}_e + \gamma_{2j} \quad (31)$$

$$W_{Net} = W_0 \quad (32)$$

$$h(\underline{\hat{x}}, RC_u) = 0 \quad (33)$$

$$g(\underline{\hat{x}}, RC_u) \leq 0 \quad (34)$$

$$\underline{x} \in \Re^n$$

In order to solve this non-linear equations system by means of the software GAMS (Rosenthal [22]), a “mute variable” (i.e. a variable which has no influence on the rest of the power plant model) is used as objective function. Nevertheless, any other method for treating with non-linear equations system may be applied; as for example the one proposed by Tarifa et al. [25], which allows selecting the decision variables and the most convenient calculation sequence in a single stage, as they demonstrated for a multiple stage flash desalination system.

As case studies, comparison between the solutions of this non-linear equations system (i.e. Problem P6) and the economic optimization problem (i.e. Problem P3) are presented, according to:

- the optimal solutions associated to actual market conditions (i.e. actual capital investment and operative costs), as listed in Table 7 for CCGT1P and in Table 8 for CCGT3P
- the optimal solutions associated to the hypothetical scenario where the capital investment on transfer area dominates the plant economics, as exemplified in Table 9 for CCGT3P

From the reported values for actual market conditions (see Table 7 and Table 8) it is determined that the mean error for the estimation of the optimal values of the design and operative variables (including the specific annual cost) is 0.40% for CCGT1P and 0.32% for CCGT3P; with maximum deviations of 1.40% and 0.91%, respectively. Meanwhile, for the hypothetical scenario where the CCGT3P plant economics is dominated by the cost of investment on transfer area (see Table 9), the mean estimation error is 0.31%, with a maximum deviation of 0.97%, and an estimation error of the specific annual cost (i.e. the objective function) of 0.10%. Similar mean error values are observed within the whole ranges of costs ratio values broaden for the here considered case studies, and for wide ranges of power production requirements.

In the search of easier ways of facing the economic optimization problem, it can be inferred that the here proposed formulation allows easily and accurately estimating the economic optima, including the optimal values of design and operative variables, for a given value of the costs ratio by simply solving the resultant system of non-linear equations and additional constraints. In addition, solving such mathematical formulation is less computationally expensive than the resolution of the original optimization problem.

6. Conclusions

Economic optima and its sensitivity to the unit costs of area and fuel are determined for the here considered power generating facilities, by means of a non-linear programming model. This analysis allows observing the behavior of both power plants design and operative variables when facing different market conditions as given by the relative weights of the costs of investment on transfer area and the operative costs due to fuel consumption. Afterwards, by comparing the economic optima with the optimal solutions of a modified thermodynamic optimization problem, useful insights into the relations between thermodynamics and economics are provided by means of the presented case studies.

Based on the optima information obtained by thermodynamic optimization, functional relationships between optimal decision variables and the specific transfer area are identified by means of a here proposed (easy to implement) procedure. Then, within the whole range of design and operative scenarios broadened for the here considered case studies, it is shown that these functional relationships are able to provide accurate estimations of the optimal values of the decision variables, including the whole set of design and operative variables associated to the power plant, such as transfer areas of the HRSG sections, power production of each turbine, fuel consumption, steam mass flow rates, operative pressures and temperatures, etc.

These instances are used to structure a novel mathematical problem, which allows obtaining accurate estimations of the economic optimal values of the power generating facility design and operative variables. This strategy allows accurately inferring the economic optima by simply solving the resultant system of non-linear equations and additional constraints, and spares the need of solving the corresponding mathematical optimization problem, which is often a difficult task due mainly to convergence and variables initialization issues.

As this here proposed mathematical formulation facilitates the acquisition of accurate estimations of the power plants design and operative variables, such optimal values can be used to efficiently initialize more complex optimization problems in the design and operation of CCGT power plants, for example if a multiperiod approach is used to evaluate the performance of the combined cycles when facing variable market conditions. Moreover, the economic optimal relationships in conjunction with the sets of equations described by the thermodynamic functional relationships can be used as self-contained reduced models of the power plants to face real time optimization problems.

Acknowledgements

The authors gratefully acknowledge the financial support of the Agencia Nacional de Promoción Cientifica y Tecnológica (ANPCyT), the Universidad Tecnológica Nacional (UTN) and the Consejo Nacional de Investigaciones Científicas y Técnicas (CONICET).

Appendix A

The description of the model of the CCGT power plant is here completed by introducing the elements included in each of the modules, for the case of CCGT3P. The model corresponding to CCGT1P can be obtained by discarding those elements that are not present in this smaller power plant.

A.1. Sets

This module is integrated by different sets, including enumeration of chemical compounds, process streams, process equipment, and saturation properties for each operative pressure level.

$QC = \{N_2, O_2, H_2O, CO_2, CH_4, C_2H_6, C_3H_8, C_4H_{10}, C_5H_{12}, C_6H_{14}\}$: Chemical Compounds

$$PS = \left\{ \begin{matrix} AA & air \\ F & fuel \\ CG & combustion\ gases \\ W & water \\ S & steam \\ WSM & water - steam\ mixture \end{matrix} \right\}$$: Process Streams

$$PE = \left\{ \begin{matrix} HE & heat\ exchangers \\ PP & pumps \\ PC & compressors \\ PT & turbines \\ COMB & combustion\ chambers \\ DEA & deaerators \\ NOD & nodes \end{matrix} \right\}$$: Process Equipment (see Figure 1 and Figure 2 for further references)

$HE = \{ECO, EVA, SH, CON, REG\}$

$ECO = \{ECO\ DEA, ECO\ LP, ECO1\ IP, ECO2\ IP, ECO1\ HP, ECO2\ HP, ECO3\ HP, \}$

$EVA = \{EVA\ DEA, EVA\ LP, EVA\ IP, EVA\ HP\}$

$SH = \{SH\ LP, SH1\ IP, SH2\ IP, SH\ HP, RH\}$

$PP = \{RP, FP\ DEA, FP\ LP, FP\ IP, FP\ HP\}$

$PC = \{AC\}$

$PT = \{GT, ST\}$

$GT = \{GT1, GT2\}$

$ST = \{ST\ LP, ST\ IP, ST\ HP\}$

$COMB = \{CC, PCC\}$

$DEA = \{DEA\}$

$NOD = \{NOD1, NOD2, \cdots\}$

$$Sat = \left\{ \begin{matrix} TCON & condenser\ operative\ pressure\ level \\ TDEA & deaerator\ operative\ pressure\ level \\ TLP & low\ pressure\ steam\ operative\ pressure\ level \\ TIP & intermediate\ pressure\ steam\ operative\ pressure\ level \\ THP & high\ pressure\ steam\ operative\ pressure\ level \end{matrix} \right\}$$: Operative Pressures Levels

A.2. Variables

Operative and design variables of the power plant are here enumerated, including selected decision variables.

T : temperature

P : pressure

X : composition (mass/ molar fraction)

h : enthalpy

s : entropy

MW : molecular weight

$\dot{m}$: mass flow rate

$\dot{Q}$: heat flow rate

U : global heat transfer coefficient

A : heat transfer area

$LMTD$: logarithmic mean temperature difference

$PinchP$: pinch point

$ApproachP$: approach point

$\dot{W}$: power production/ consumption

The following additional subindexes apply to the variables enumeration.

cf : cold fluid

hf : hot fluid

ce : cold end

he : hot end

in : inlet process stream

out : outlet process stream

i : isentropic evolution

p : polytropic evolution

$Loss$: heat loss

zr : z-th chemical reaction

A.3. Input Data

Fixed parameters adopted as input data are taken from general and technical literature, technical specifications from equipment manufacturers, etc. Input data here used is listed in Table 10.

A.4. Properties

Enthalpy, entropy and other properties (not listed here) of each fluid stream are calculated by considering their dependence on temperature, pressure and compositions.

$h_{PS} = f(T_{PS}, P_{PS}, X_{PS,QC})$: Enthalpy Correlation (A.1)

$s_{PS} = f\left(T_{PS}, P_{PS}, X_{PS,QC}\right)$: Entropy Correlation (A.2)

In addition, a standard correlation is used to estimate the steam saturation pressure.

$P_{Sat} = f(T_{Sat})$: Saturation Pressure Correlation (A.3)

The thermodynamic properties correlations can be obtained from the standard literature (for example, correlations produced by IAPWS [26, 27] are used to calculate water and steam properties, while correlations given in Perry [28] are used to predict some gas properties).

A.5. Equipment

For each unit operation, mass and energy balances and design equations are included within this module.

A.5.1. Heat Exchangers

Mass and energy balances are applied to every HRSG section, as well as the condenser and the regenerator. Design equations, which include the heat transfer area, the logarithmic mean temperature difference and the pressure loss calculation, for each heat transfer section, are also considered.

$\dot{Q}_{HE} = \dot{m}_{HE,cf} \,.\, \Delta h_{HE,cf} = \dot{m}_{HE,hf} \,.\, \Delta h_{HE,hf}$: Mass and Energy Balances (A.4)

$\dot{Q}_{HE} = U_{HE} \,.\, A_{HE} \,.\, LMTD_{HE}$: Heat Transfer Area Calculation (A.5)

$LMTD_{HE} = \frac{\Delta T_{HE,ce} - \Delta T_{HE,he}}{ln\left(\Delta T_{HE,ce}/\Delta T_{HE,he}\right)}$: Logarithmic Mean Temperature Difference Calculation (A.6)

$\Delta P_{HE,j} = \Delta P_{HE,j,in} - \Delta P_{HE,j,out} \quad , \quad j = cf, hf$: Pressure Loss Calculation (A.7)

In addition, for the evaporator sections of the HRSG, calculation of the pinch point and the approach point is included.

$PinchP_{EVA} = T_{EVA,hf,out} - T_{EVA,cf,out}$: Pinch Point Calculation (A.8)

$ApproachP_{EVA} = T_{EVA,cf,out} - T_{EVA,cf,in}$: Approach Point Calculation (A.9)

A.5.2. Pumps

Pumps consume power for condensate recirculation, to force feed water into the HRSG, etc.

$\dot{W}_{PP} = \dot{m}_{PP} \,.\, \Delta h_{PP}$: Mass and Energy Balances (A.10)

For the process pumps, isentropic evolutions are considered, as the error introduced in the final net power production is despicable.

$s_{PP,out} = s_{PP,in}$: Isentropic Evolution (A.11)

A.5.3. Compressors

Expressions of the isentropic efficiency are used to account for the irreversibilities of the compression processes, allowing to accurately compute the power consumption of each unit.

$\dot{W}_{PC} = \dot{m}_{PC} \,.\, \Delta h_{PC}$: Mass and Energy Balances (A.12)

$\eta_{PC,i} = \left[\left(P_{PC,out}/P_{PC,in} \right)^{\frac{kp_{PC}-1}{kp_{PC}}} - 1 \right] \Big/ \left[\left(P_{PC,out}/P_{PC,in} \right)^{\frac{kp_{PC}-1}{\eta_{PC,p}\,.\,kp_{PC}}} - 1 \right]$: Isentropic Efficiency (A.13)

$\eta_{PC,i} = \frac{\Delta h_{PC,i}}{\Delta h_{PC}}$: Isentropic Efficiency (A.14)

A.5.4. Turbines

Expressions of the isentropic efficiency are used to account for the irreversibilities of the expansion processes, allowing to accurately compute the power production of each unit.

$\dot{W}_{PT} = \dot{m}_{PT} \,.\, \Delta h_{PT}$: Mass and Energy Balances (A.15)

$\eta_{PT,i} = \left[\left(P_{PT,in}/P_{PT,out} \right)^{\frac{1-kp_{PT}}{kp_{PT}}} - 1 \right] \Big/ \left[\left(P_{PT,in}/P_{PT,out} \right)^{\frac{1-kp_{PT}}{\eta_{PT,p}\,.\,kp_{PT}}} - 1 \right]$: Isentropic Efficiency (A.16)

$\eta_{PT,i} = \frac{\Delta h_{PT}}{\Delta h_{PT,i}}$: Isentropic Efficiency (A.17)

A.5.5. Combustion Chambers

A mass balance for each chemical compound and a global energy balance, which takes into account heat losses, are considered at each combustion chamber.

$X_{COMB,QC,out} \,.\, \dot{m}_{COMB,out} = \sum_{in} X_{COMB,QC,in} \,.\, \dot{m}_{COMB,in} + \sum_{zr} \dot{r}_{COMB,QC,zr}$: Mass Balances (A.18)

$\dot{m}_{COMB,out} \,.\, h_{COMB,out} + \dot{Q}_{COMB,Loss} = \sum_{in} \dot{m}_{COMB,in} \,.\, h_{COMB,in}$: Energy Balance (A.19)

$\Delta P_{COMB} = \Delta P_{COMB,in} - \Delta P_{COMB,out}$: Pressure Loss Calculation (A.20)

A.5.6. Deaerator

In the deaerator, steam is used for incondensable gases elimination. Mass and energy balances are considered for this unit.

$\sum_{out} \dot{m}_{DEA,out} = \sum_{in} \dot{m}_{DEA,in}$: Mass Balance (A.21)

$\sum_{out} \dot{m}_{DEA,out} \,.\, h_{DEA,out} = \sum_{in} \dot{m}_{DEA,in} \,.\, h_{DEA,in}$: Energy Balance (A.22)

A.5.7. Nodes

Mass and energy balances are considered for each addition and division node.

$\sum_{out} \dot{m}_{NOD,out} = \sum_{in} \dot{m}_{NOD,in}$: Mass Balance (A.23)

$\sum_{out} \dot{m}_{NOD,out} \,.\, h_{NOD,out} = \sum_{in} \dot{m}_{NOD,in} \,.\, h_{NOD,in}$: Energy Balance (A.24)

A.6. Assignments

Groups of linear constraints are here defined to assign streams to equipment inputs and outputs, including all the associated properties; as well as to relate streams to other streams. An example of each is shown below.

$\dot{m}_{PC} = \dot{m}_{AA1}$: Stream to Equipment Assignment Linear Constraint (A.25)

$\dot{m}_{AA2} = \dot{m}_{AA1}$: Stream to Stream Assignment Linear Constraint (A.26)

A.7. Global Balances

Global decision variables are here computed, including the net power production and the net transfer area.

A.7.1. Net Power Production and Thermal Efficiency Calculation

The net energy consumed by the power plant is computed as the total energy supplied by the fuel.

$\dot{Q}_{Net} = \sum_{COMB} \dot{m}_{COMB,F} \,.\, LHV_{COMB,F}$: Net Energy Consumption (A.27)

The net power produced by the gas turbine is computed as the difference of the power generated by the turbines and the power consumed by the compressors.

$\dot{W}_{GT,Net} = \sum_{GT} \dot{W}_{GT} - \sum_{PC} \dot{W}_{PC}$: Gas Turbine Net Power Production (A.28)

The net power produced by the steam turbine is computed as the difference of the power generated by the turbines and the power consumed by the pumps.

$\dot{W}_{ST,Net} = \sum_{ST} \dot{W}_{ST} - \sum_{PP} \dot{W}_{PP}$: Steam Turbine Net Power Production (A.29)

The net power production of the power plant is computed as the summation of the net power generated by the gas and steam turbines.

$\dot{W}_{Net} = \dot{W}_{GT,Net} + \dot{W}_{ST,Net}$: Net Power Production (A.30)

A.7.2. Net Transfer Area Calculation

The net transfer area necessary for each operative pressure level is computed as the summation of the transfer areas of economizers, evaporator and superheaters for such operative pressure level.

$A_{DEA,Net} = \sum_{DEA} A_{HE}$: Net Transfer Area for Deaerator Pressure Level (A.31)

$A_{LP,Net} = \sum_{LP} A_{HE}$: Net Transfer Area for Low Pressure Level (A.32)

$A_{IP,Net} = \sum_{IP} A_{HE}$: Net Transfer Area for Intermediate Pressure Level (A.33)

$A_{HP,Net} = \sum_{HP} A_{HE}$: Net Transfer Area for High Pressure Level (A.34)

The HRSG net transfer area is calculated as the summation of the transfer areas necessary for each operative pressure level.

$A_{HRSG,Net} = A_{DEA,Net} + A_{LP,Net} + A_{IP,Net} + A_{HP,Net}$: Net Transfer Area for HRSG (A.35)

The net transfer area is computed as the summation of the transfer areas of the HRSG and the associated condenser.

$A_{Net} = A_{HRSG,Net} + A_{CON}$: Net Transfer Area (A.36)

A.8. Technical Constraints

In order to set useful boundaries to circumscribe a feasible operation region according to practical experience, the following technical (inequality) constraints are considered in the model:

- Minimum and Maximum Approach Point, to guarantee no water evaporation in the economizer and to avoid thermal shock at evaporator entry, respectively

$ApproachP_{min} \leq ApproachP_{EVA} \leq ApproachP_{max}$: Approach Point Constraints (A.37)

- Minimum and Maximum Pinch Point, to secure reasonable practical values of the HRSG heat transfer area

$PinchP_{min} \leq PinchP_{EVA} \leq PinchP_{max}$: Pinch Point Constraints (A.38)

- Maximum steam pressure in the HRSG, to assure operation within normal parameters

$P_{Sat} \leq P_{Sat,max}$: Operative Pressures Constraints (A.39)

- Minimum operative pressure of the condenser, fixed by minimum temperature of available cooling water

$P_{TCON} \geq P_{TCON,min}$: Condenser Operative Pressure Constraint (A.40)

- Maximum gas temperature at HRSG inlet, to prevent materials deterioration

$T_{HRSG,in} \leq T_{HRSG,max}$: HRSG Inlet Temperature Constraint (A.41)

- Minimum gas temperature at HRSG discharge, to prevent corrosion due to water condensation

$T_{HRSG,out} \geq T_{HRSG,min}$: HRSG Discharge Temperature Constraint (A.42)

- Maximum temperature at turbine inlet, determined by the materials resistance

$T_{PT,in} \leq T_{PT,max}$: Turbine Inlet Temperature Constraints (A.43)

- Minimum temperature difference at superheater exit, to assure operation within normal parameters

$T_{SH,hf,in} - T_{SH,cf,out} \geq \Delta T_{SH,min}$: Superheater Temperature Difference Constraints (A.44)

- Minimum temperature difference al regenerator exit, to assure operation within normal parameters

$T_{REG,hf,in} - T_{REG,cf,out} \geq \Delta T_{REG,min}$: Superheater Temperature Difference Constraints (A.45)

- Minimum and Maximum steam quality at steam turbine discharge, to achieve normal operation of the turbine

$X_{ST,WSM,min} \leq X_{ST,WSM,out} \leq X_{ST,WSM,max}$: Discharge Steam Quality Constraints (A.46)

- Maximum compression ratio in the air compressor, to achieve normal operation of the compressor

$\frac{P_{PC,out}}{P_{PC,in}} \leq CR_{PC,max}$: Compression Ratio Constraints (A.47)

A.9. Logical Constraints

Generally, some inequalities must be defined to secure all the operative variables adopt feasible physical values. Nevertheless, as GAMS is used as modeling software, this can be accomplished, for example, by defining the variables over restricted domains (i.e. as positive or negative variables).

Appendix B

B.1. Evolution of the Optimal Decision Variables for CCGT1P

In this section, characteristics of the evolution of the decision variables associated to CCGT1P are analyzed.

B.1.1. Distribution of the Power Generation

The power ratio exhibits a decreasing trend as the specific transfer area increases. In other words, for a fixed power generation capacity, as more area is assigned to the power plant, a bigger percentage of the energy should be produced by the steam turbine in order to achieve the maximum feasible value of the thermal efficiency.

For CCGT1P, the power ratio decreases from 3.45 at 170 m^2/MW to 2.42 at 260 m^2/MW, which represents a diminution of about -30%.

B.1.2. Distribution of the Heat Transfer Area

Distribution of the total hear transfer area is here done in a sequential way. Considering the hot source- cold sink structure proposed by Vargas and Bejan [17] for the fundamental problem of matching thermodynamically two streams, assignment of transfer area to the HSRG (hot source of the steam cycle) and the condenser (cold sink of the power plant) is done in a first instance.

It can be observed that the HRSG area allocation ratio exhibits a positive bias, although the percentage variation of its optimal value is only 0.20% from one end to the other (i.e. from 0.8776 at 170 m^2/MW to 0.8794 at 260 m^2/MW). Then, 87-88% of the total transfer area is always assigned to the HRSG in order to transfer the remaining heat of the gas turbine exhaust gas to the steam cycle.

In second instance, distribution of transfer area among the HRSG sections is executed. Here, the economizer area exhibits an increasing trend, while the evaporator and the superheater area fractions decrease as the specific transfer area increases.

A larger economizer is necessary for conditioning the increasing water flow rate (as will be shown further ahead) necessary for achieving the optimal profiles of power production, as more transfer area is assigned to the power plant. In opposition, increasingly smaller evaporator and superheater are needed, as their operative temperatures become higher (as will be shown further ahead), and therefore both the latent heat and the superheating temperature difference result smaller.

For the interest range of values of the specific transfer area, the economizer area allocation ratio varies from 0.1808 to 0.3325 (84%), while the evaporator area fraction decreases from 0.7359 to 0.5874 (-20%), and the superheater area fraction diminishes from 0.0833 to 0.0799 (-4%).

B.1.3. Gas Flow Pressures

The compression ratio decreases from almost 20 at 170 m^2/MW to nearly 14 at 260 m^2/MW, which represents a diminution of -29%. This decrement of the compression ratio accompanies the decrease of the power generation fraction which the gas turbine must fulfill in an optimal way in order to achieve the maximum value of the technical performance indicator. This indicates that for high values of the specific transfer area, the steam turbine is able to generate power more efficiently that the gas turbine, and therefore it should be preferred for addressing the extra power demand.

B.1.4. HRSG Operative Temperatures

As previously mentioned, the evaporator operative temperature presents an increasing trend respect to the specific transfer area. Along with such increments, the amount of heat necessary for steam generation diminishes, as the latent heat does.

For CCGT1P, the operative temperature ratio increases from 1.77 at 170 m^2/MW to 1.87 at 260 m^2/MW, which represents a growth of about 5.3%.

B.1.5. Fuel Consumption per Unit of Generated Power

As a larger specific transfer area is assigned to the power plant, the system is able to generate power in a more efficient manner and, as previously exposed, the power generation increasingly shifts from the gas turbine to the steam turbine. Then, the fuel requirement per unit of power generated by the gas turbine becomes smaller by -3.5% (i.e. decreases from 1.96 to 1.89) within the interest range of specific transfer area values.

B.1.6. Relations among Flow Rates

The air flow rate relation diminishes from around 37 for a specific transfer area value of 170 m^2/MW down to nearly 33 for a specific transfer area value of 260 m^2/MW, which sums up a total variation of -9%. This variation implies a diminution of the required excess of air, which translates into a smaller power generation in the gas turbine and a larger amount of heat delivered to the steam cycle.

Increasing the output of the steam turbine is ultimately accomplished as the steam flow rate relation goes from 6.01 at 170 m^2/MW to 6.58 at 260 m^2/MW, which represents a percentage variation of 9.6%.

B.2. Evolution of the Optimal Decision Variables for CCGT3P

In this section, characteristics of the families of optimal solutions regarding the optimal values of the decision variables associated to CCGT3P are analyzed.

It can be noticed that reported values of the thermal efficiency for CCGT3P result higher than the ones obtained in the industrial practice, as the model variables are allowed to adjust their values within wide ranges, which enables to reach further improvements of the system performance. In addition, for a three pressure levels combined cycle, Franco and Casarosa [19] stated that joining HRSG optimization with postcombustion and regeneration can lead the efficiency of the whole plant to the value of 65%, for a turbine inlet temperature of 1500 K. Similar considerations were exposed by Bassily [12], mainly regarding the HRSG operative parameters.

B.2.1. Distribution of the Power Generation

Similarly to CCGT1P, the power production distribution has a negative bias, as it decreases from 1.095 at 360 m^2/MW to 1.072 at 480 m^2/MW.

In this case, variation of the power ratio within the interest range of specific transfer area values reaches only -2.1%, against a value of -30% observed for CCGT1P. Then, similar trends are observed for both power plants, although the effect is much less noticeable for the large scale system.

B.2.2. Distribution of the Heat Transfer Area

Distribution of the total hear transfer area is here sequentially done in three steps.

First, area is assigned either to the HRSG or to the condenser (i.e. hot source vs. cold sink, see Vargas and Bejan [17]).

It can be observed that the HRSG area allocation ratio exhibits a positive bias, and that the percentage variation of its optimal value reaches 1.15% (i.e. from 0.4784 at 360 m^2/MW to 0.4839 at 480 m^2/MW) for the interest range of specific transfer area values. Such variation results almost six times larger than the correspondent one associated to CCGT1P. Nevertheless, only about half of the available transfer area is assigned to the HRSG, as the cooling requirements of the large scale power plant are much larger than the small scale cycle ones.

Second, the area assigned to the HRSG is either allocated for conditioning the feed water to the deaerator, to address the heat transfer requirements of the low, intermediate and high pressure operative levels, or for accomplishing reheating of the steam between the high and intermediate pressure stages of the steam turbine.

As the specific transfer area grows, more area is allocated in the low and high pressures sections, in detriment of the transfer area fractions of the deaerator, intermediate pressure and reheater sections. Observed variations area as follows:

- For DEA operative pressure level, from 0.1902 at 360 m^2/MW to 0.1217 at 480 m^2/MW (i.e. -36%)
- For LP operative pressure level, from 0.0852 at 360 m^2/MW to 0.0926 at 480 m^2/MW (i.e. 8.7%)
- For IP operative pressure level, from 0.2351 at 360 m^2/MW to 0.2280 at 480 m^2/MW (i.e. -3%)
- For HP operative pressure level, from 0.4363 at 360 m^2/MW to 0.5138 at 480 m^2/MW (i.e. 18%)
- For RH section, from 0.0531 at 360 m^2/MW to 0.0432 at 480 m^2/MW (i.e. -19%)

Lastly, distribution of transfer area within each pressure operative level is carried out, as transfer area is assigned to economizers, evaporators and superheaters.

Regarding the economizer area fraction, dissimilar behaviors are observed. Economizers associated to the DEA, IP and HP operative levels become smaller as the available specific transfer area enlarges. The inverse trend is observed for the economizer linked to the LP operative level. A summary of the evolution of the economizers area fraction is presented next:

- Economizer for DEA operative pressure level, from 0.3922 at 360 m^2/MW to 0.5280 at 480 m^2/MW (i.e. 35%)
- Economizer for LP operative pressure level, from 0.0116 at 360 m^2/MW to 0.0086 at 480 m^2/MW (i.e. -25%)
- Economizer for IP operative pressure level, from 0.0937 at 360 m^2/MW to 0.1082 at 480 m^2/MW (i.e. 16%)
- Economizer for HP operative pressure level, from 0.3956 at 360 m^2/MW to 0.4607 at 480 m^2/MW (i.e. 16%)

The evaporators area allocation ratio diminishes within the interest range of specific transfer area values, for all the HRSG operative pressures levels, as their operative temperatures become higher (as will be shown further ahead) and the latent heats result smaller. A summary of the evolution of the evaporators area fraction is presented next:

- Evaporator for DEA operative pressure level, from 0.6078 at 360 m^2/MW to 0.4717 at 480 m^2/MW (i.e. -22%)
- Evaporator for LP operative pressure level, from 0.9327 at 360 m^2/MW to 0.8000 at 480 m^2/MW (i.e. -14%)
- Evaporator for IP operative pressure level, from 0.7302 at 360 m^2/MW to 0.6778 at 480 m^2/MW (i.e. -7%)
- Evaporator for HP operative pressure level, from 0.3655 at 360 m^2/MW to 0.3196 at 480 m^2/MW (i.e. -13%)

Dissimilar trends are also observed respect to superheaters area allocation ratio. Size of superheaters linked to LP and IP operative levels increase as the specific transfer area becomes larger; while the opposite behavior is observed regarding the superheater associated to the HP operative level. A summary of the evolution of the superheaters area fraction is presented next:

- Superheater for LP operative pressure level, from 0.0557 at 360 m^2/MW to 0.1909 at 480 m^2/MW (i.e. 243%)
- Superheater for IP operative pressure level, from 0.1706 at 360 m^2/MW to 0.2135 at 480 m^2/MW (i.e. 21%)
- Superheater for HP operative pressure level, from 0.2388 at 360 m^2/MW to 0.2193 at 480 m^2/MW (i.e. -8%)

Note that mixed tendencies observed for the economizers and superheaters area allocation ratios are caused by the utilization of parallel transfer sections in the HRSG, as the available heat must be distributed simultaneously to several sections with different requirements.

B.2.3. Gas Flow Pressures

The expansion ratio decrease about -0.13%, from 5.445 at 360 m^2/MW to 5.437 at 480 m^2/MW for GT1, and from 5.093 at 360 m^2/MW to 5.086 at 480 m^2/MW for GT2.

Decrements of the expansion ratios at CCGT3P gas turbines are caused by the diminution of the power generation fraction to be optimally fulfilled by the gas turbines, forced by the increment of the steam cycle efficiency caused by the additional specific transfer area provided to the large scale power plant.

B.2.4. HRSG Operative Temperatures

Operative temperatures of the DEA, LP, IP and HP evaporators present increasing trends respect to the specific transfer area. Nevertheless, only the relation between HP and IP operative pressures increases as the specific transfer area becomes larger, from 1.265 at 360 m^2/MW to 1.313 at 480 m^2/MW (which represents a growth of about 3.8%). Meanwhile, IP- LP and LP- DEA operative temperatures remain invariable, at values of 1.057 and 1.102, respectively.

Along with increments of the evaporators operative temperatures, the amount of heat necessary for steam generation diminishes, as the latent heat does.

B.2.5. Fuel Consumption per Unit of Generated Power

For CCGT3P, the optimal value of the fuel requirement of each combustion chamber per unit of power generated by the gas turbine remain constant (at values of 1.120 and 0.910, respectively) within the interest range of specific transfer area values. Then, contrarily to the behavior observed for CCGT1P case, shift of the power generation from the gas turbine to the steam turbine seems not to affect the specific fuel consumption.

B.2.6. Relations among Flow Rates

Similarly to the behavior of the specific fuel consumption for CCGT3P, the air flow rate ratio remains invariable at a constant value of 23.2.

For the large scale power plant, increment of the steam turbine power output is accomplished with decreasing values of the steam flow rate relations. A summary of the evolution of the steam flow rate relations for each operative pressure level is presented next

- Steam flow rate relation for DEA operative pressure level, from 105.1 at 360 m^2/MW to 104.4 at 480 m^2/MW (i.e. -0.7%)

- Steam flow rate relation for LP operative pressure level, from 4.9 at 360 m^2/MW to 4.5 at 480 m^2/MW (i.e. -7.8%)
- Steam flow rate relation for IP operative pressure level, from 23.5 at 360 m^2/MW to 23.26 at 480 m^2/MW (i.e. -1.1%)
- Steam flow rate relation for HP operative pressure level, from 76.71 at 360 m^2/MW to 76.72 at 480 m^2/MW (i.e. -0.1%)

References

[1] M. V. Biezma, J. R. San Cristóbal, Investment criteria for the selection of cogeneration plants- a state of the art review, Appl. Therm. Eng. 26 (2006) 583-588

[2] D. S. Remer, A. P. Nieto, A compendium and comparison of 25 project evaluation techniques. Part 1: Net present value and rate of return methods, Int. J. Prod. Econ. 42 (1995) 79-96

[3] D. S. Remer, A. P. Nieto, A compendium and comparison of 25 project evaluation techniques. Part 2: Ratio, payback, and accounting methods, Int. J. Prod. Econ. 42 (1995) 101-129

[4] J. Kotowicz, L. Bartela, The influence of economic parameters on the optimal values of the design variables of a combined cycle plant, Energy 35 (2010) 911–919

[5] C. Poma, V. Verda, S. Consonni, Design and performance evaluation of a waste-to-energy plant integrated with a combined cycle, Energy 35 (2010) 786–793

[6] S. F. Mussati, P. A. Aguirre, N. Scenna, Thermodynamic approach for optimal design of heat and power plants. Relationship between thermodynamic and economic solutions, Lat. Am. Appl. Res. 36 (2006) 329–335

[7] A. Franco, C. Casarosa, Thermoeconomic evaluation of the feasibility of highly efficient combined cycle power plants, Energy 29 (2004) 1963–1982

[8] M. Valdés, M. D. Durán, A. Rovira, Thermoeconomic optimization of combined cycle gas turbine power plants using genetic algorithms, Appl. Therm. Eng. 23 (2003) 2169–2182

[9] M. A. Rosen, I. Dincer, Exergoeconomic analysis of power plants operating on various fuels, Appl. Therm. Eng. **23** (2003) 643-658

[10] A. Franco, N. Giannini, A General Method for the Optimum Design of Heat Recovery

Steam Generators, Energy 31 (2006) 3342-3361

[11] M. Valdés, J.L. Rapún, Optimization of Heat Recovery Steam Generators for Combined Cycle Gas Turbine Power Plants, Appl. Therm. Eng. 21 (2000) 1149-1159

[12] A.M. Bassily, Modeling, numerical optimization, and irreversibility reduction of a triple-pressure reheat combined cycle, Energy 32 (2007) 778–794

[13] N. Woudstra, T. Woudstra, A. Pirone, T. Van der Stelt, Thermodynamic evaluation of combined cycle plants, Energy Convers. Manage. 51 (2010) 1099–1110

[14] N.J. Scenna, P. Aguirre, Optimal thermodynamic synthesis of dual-purpose desalination plants. Extraction vs. back pressure turbines, Desalination 81 Issues 1-3 (1991) 419-436

[15] D. Tondeur, E. Kvaalen, Equipartition of entropy production. An optimality criterion for transfer and separation processes, Ind. Eng. Chem. Res. 26 (1987) 50–56

[16] L. Nummedal, S. Kjelstrup, Equipartition of forces as a lower bound on the entropy production in heat exchange, Int. J. Heat Mass Tran. 44 (2001) 2827-2833

[17] J.V.C. Vargas, A. Bejan, Thermodynamic optimization of the match between two streams with phase change, Energy 25 (2000) 15–33

[18] E. Godoy, N. Scenna, S. Benz, Families of Optimal Thermodynamic Solutions for Combined Cycle Gas Turbine (CCGT) Power Plants, Appl. Therm. Eng. 30 (2010) 569-576

[19] A. Franco, C. Casarosa, On some perspectives for increasing the efficiency of combined cycle power plants, Appl. Therm. Eng. 22 (2002) 1501-1518

[20] GE, Gas Turbine and Combined Cycle Products, GE Power Systems, Atlanta, USA, 2010. See also: http://www.ge-energy.com

[21] Siemens, Siemens Combined Cycle - Reference Power Plant SCC5-4000F 2x1, Siemens AG, Erlangen, Germany, 2008. See also: http://www.energy.siemens.com

[22] R. E. Rosenthal, GAMS. A User Guide, GAMS Development Corporation, Washington DC, USA. See also: http://www.gams.com/docs/document.htm

[23] A. Drud, CONOPT, ARKI Consulting and Development A/S, Bagsvaerd, Denmark. See also: http://www.gams.com/docs/document.htm

[24] P. Regulagadda, I. Dincer, G.F. Naterer, Exergy analysis of a thermal power plant with measured boiler and turbine losses, Appl. Therm. Eng. 30 (2010) 970–976

[25] E. Tarifa, D. Humana, S. Franco, N. J. Scenna, A new method to process algebraic

equation systems used to model a MSF desalination plant, Desalination 166 (2004) 113-121

[26] IAPWS, Revised Supplementary Release on Saturation Properties of Ordinary Water Substance, IAPWS, St. Petersburg, Russia, 1992. See also: http://www.iapws.org

[27] IAPWS, Revised Release on IAPWS Industrial Formulation 1997 for the Thermodynamic Properties of Water and Steam, IAPWS, Lucerne, Switzerland. 2007. See also: http://www.iapws.org

[28] J. Perry, Chemical Engineers Handbook. McGraw-Hill, Mexico, 1995

List of Tables

Table 1: Comparison of CCGT1P and a Commercially Available Small Scale Power Plant

Table 2: Comparison of CCGT3P and a Commercially Available Large Scale Power Plant

Table 3: Definition of Practical Interest Technical Ratios

Table 4: Values of the Adjustment Parameters for Ratios associated to CCGT1P

Table 5: Values of the Adjustment Parameters for Ratios associated to CCGT3P

Table 6: Values of the Adjustment Parameters $\delta_{1A_e}, \delta_{2A_e}, \delta_{3A_e}$ for the Economic Optimal Relationships of the Specific Transfer Areas

Table 7: Values of Selected Design and Operative Variables for CCGT1P – Comparison for Section 5, considering Actual Market Conditions

Table 8: Values of Selected Design and Operative Variables for CCGT3P – Comparison for Section 5, considering Actual Market Conditions

Table 9: Values of Selected Design and Operative Variables for CCGT3P – Comparison for Section 5, considering Plant Economics Dominated by Cost of Investment on Transfer Area

Table 10: Input Data

List of Figures

Figure 1: CCGT1P Power Plant Diagram

Figure 2: CCGT3P Power Plant Diagram

Figure 3: Optimal Evolution of the Thermal Efficiency for a Wide Range of Specific Transfer Areas

Figure 4: Application Example of the Functional Relationships for the HRSG Area Allocation Ratio of CCGT3P

Figure 5: Optimal Evolution of the Specific Annual Cost for a Wide Range of Costs Ratio Values

Figure 6: Costs Distribution for CCGT1P

Figure 7: Costs Distribution for CCGT3P

Figure 8: Specific Annual Cost Associated to the Thermodynamic Optima and Optimal Specific Annual Cost for CCGT1P

Figure 9: Specific Annual Cost Associated to the Thermodynamic Optima and Optimal Specific Annual Cost for CCGT3P

Figure 10: CCGT1P Specific Transfer Area – Optimal Values vs. Economic Optimal Relationship

Figure 11: CCGT3P Specific Transfer Area – Optimal Values vs. Economic Optimal Relationship

Table 1

Table 1: Comparison of CCGT1P and a Commercially Available Small Scale Power Plant

Variable	CCGT1P	MS9001FA 1x1 from GE Power Systems
Gas Turbine Net Power Output (MW)	272.5	255.6
Steam Turbine Design Power (MW)	127.5	135.2
Power Plant Production Capacity (MW)	400	390.8
Compression Ratio	14.8:1	15.4:1
Exhaust Mass Flow (kg/s)	780	624
Exhaust Temperature (K)	768	882
Thermal Efficiency (%)	52.7	56.7
Iteration Count	13	
Resolution Time (s)	0.598	

Table 2

Table 2: Comparison between CCGT3P and a Commercially Available Large Scale Power Plant

Variable	CCGT3P	SCC5-4000F 2x1 from Siemmens
Gas Turbine Net Power Output (MW)	348	288
Steam Turbine Design Power (MW)	304	272
Power Plant Production Capacity (MW)	1000	848
Compression Ratio	30:1	18.2:1
Exhaust Mass Flow (kg/s)	630	688
Exhaust Temperature (K)	900	850
Thermal Efficiency (%)	63.6	58.5
Iteration Count	35	
Resolution Time (s)	0.133	

Table 3

Table 3: Definition of Practical Interest Technical Ratios

Symbol	Definition	Formula
A_e	Specific Transfer Area	$\frac{A_{Net}}{\dot{W}_{Net}}$
PR	Power Production Distribution	$\frac{\dot{W}_{GT,Net}}{\dot{W}_{ST,Net}}$
AAR_{HRSG}	Area Allocation Ratio – HRSG	$\frac{A_{HRSG,Net}}{A_{Net}}$
$AARO_j$	Area Allocation Ratio – j Operative Pressure Level	$\frac{A_{j,Net}}{A_{HRSG,Net}}$, $j = DEA, LP, IP, HP, RH$
$AAROS_{k,j}$	Area Allocation Ratio – k Transfer Section at j Operative Pressure Level	$\frac{A_{k,j}}{A_{j,Net}}$, $k = ECO, EVA, SH$; $j = DEA, LP, IP, HP$
CR_j	Compression Ratio – Air Compressor	$\frac{P_{j,out}}{P_{j,in}}$, $j = AC$
ER_j	Expansion Ratio – Gas Turbine j	$\frac{P_{j,in}}{P_{j,out}}$, $j = GT1, GT2$
$TR_{j,k}$	Operative Temperature Ratio – Operative Temperature at Level j vs. Operative Temperature at Level k	$\frac{T_{Sat,j}}{T_{Sat,k}}$, $j = DEA, LP, IP, HP$; $k = DEA, LP, IP, HP$, $j \neq k$
MF_j	Specific Fuel Consumption – j Combustion Chamber	$\frac{\dot{m}_{j,F,in}. LHV}{\dot{W}_{GT,Net}}$, $j = CC, PCC$
MA	Air Flow Rate Relation	$\frac{\dot{m}_{PC,AA,in}}{\dot{m}_{CC,F,in} + \dot{m}_{PCC,F,in}}$
MS_j	Steam Flow Rate Relation – j Operative Pressure Level	$\frac{\dot{m}_{EVA,j,out}}{\dot{m}_{CC,F,in} + \dot{m}_{PCC,F,in}}$, $j = DEA, LP, IP, HP$

Table 4

Table 4: Values of the Adjustment Parameters for Ratios associated to CCGT1P

Ratio	Indexes Values	Coefficient γ_{1j}	Coefficient γ_{2j}
PR		-1.138 x 10^{-2}	5.382 x 10^{0}
AAR_{HRSG}		2.013 x 10^{-5}	8.741 x 10^{-1}
	$k = ECO$, $j = LP$	1.686 x 10^{-3}	-1.059 x 10^{-1}
$AAROS_{k,j}$	$k = EVA$, $j = LP$	-1.650 x 10^{-3}	1.016 x 10^{0}
	$k = SH$, $j = LP$	-3.766 x 10^{-5}	8.973 x 10^{-2}
CR_j	$j = AC$	-6.414 x 10^{-2}	3.077 x 10^{1}
$TR_{j,k}$	$j = LP$, $k = T_0$	1.049 x 10^{-3}	1.596 x 10^{0}
MF_j	$j = CC$	-7.560 x 10^{-4}	2.084 x 10^{0}
MA		-3.710 x 10^{-2}	4.311 x 10^{1}
MS_j	$j = LP$	6.398 x 10^{-3}	4.921 x 10^{0}

Table 5

Table 5: Values of the Adjustment Parameters for Ratios associated to CCGT3P

Ratio	Indexes Values	Coefficient γ_{1j}	Coefficient γ_{2j}
PR		-1.924 x 10^{-4}	1.164 x 10^{0}
AAR_{HRSG}		4.601 x 10^{-5}	4.619 x 10^{-1}
$AARO_j$	$j = DEA$	-5.708 x 10^{-4}	3.957 x 10^{-1}
	$j = LP$	6.201 x 10^{-5}	6.268 x 10^{-2}
	$j = IP$	-5.895 x 10^{-5}	2.563 x 10^{-1}
	$j = HP$	6.451 x 10^{-4}	2.041 x 10^{-1}
	$j = RH$	-8.293 x 10^{-5}	8.296 x 10^{-2}
$AAROS_{k,j}$	$k = ECO \quad , \quad j = DEA$	1.132 x 10^{-3}	-1.532 x 10^{-2}
	$k = EVA \quad , \quad j = DEA$	-1.134 x 10^{-3}	1.016 x 10^{0}
	$k = ECO \quad , \quad j = LP$	-2.448 x 10^{-5}	2.040 x 10^{-2}
	$k = EVA \quad , \quad j = LP$	-1.106 x 10^{-3}	1.331 x 10^{0}
	$k = SH \quad , \quad j = LP$	1.127 x 10^{-3}	-3.500 x 10^{-1}
	$k = ECO \quad , \quad j = IP$	1.214 x 10^{-4}	4.999 x 10^{-2}
	$k = EVA \quad , \quad j = IP$	-4.366 x 10^{-4}	8.874 x 10^{-1}
	$k = SH \quad , \quad j = IP$	3.121 x 10^{-4}	6.368 x 10^{-2}
	$k = ECO \quad , \quad j = HP$	5.427 x 10^{-4}	2.002 x 10^{-1}
	$k = EVA \quad , \quad j = HP$	-3.830 x 10^{-4}	5.034 x 10^{-1}
	$k = SH \quad , \quad j = HP$	-1.629 x 10^{-4}	2.975 x 10^{-1}
ER_j	$j = GT1$	-6.495 x 10^{-5}	5.468 x 10^{0}
	$j = GT2$	-5.703 x 10^{-5}	5.113 x 10^{0}

	$j = LP \quad , \quad k = DEA$	0.000×10^{0}	1.058×10^{0}
$TR_{j,k}$	$j = IP \quad , \quad k = LP$	0.000×10^{0}	1.102×10^{0}
	$j = HP \quad , \quad k = IP$	4.005×10^{-4}	1.121×10^{0}
MF_j	$j = CC$	0.000×10^{0}	1.122×10^{0}
	$j = PCC$	0.000×10^{0}	9.098×10^{-1}
MA		0.000×10^{0}	2.317×10^{1}
	$j = DEA$	-6.032×10^{-3}	1.073×10^{2}
MS_j	$j = LP$	-3.166×10^{-3}	6.033×10^{0}
	$j = IP$	-2.162×10^{-3}	2.430×10^{1}
	$j = HP$	-7.061×10^{-4}	7.696×10^{1}

Table 6

Table 6: Values of the Adjustment Parameters $\delta_{1A_e}, \delta_{2A_e}, \delta_{3A_e}$ for the Economic Optimal Relationships of the Specific Transfer Areas

	δ_{1A_e}	δ_{2A_e}	δ_{3A_e}
CCGT1P	251.2	-155.9	-0.01153
CCGT3P	475.6	-32.41	-0.6023

Table 7

Table 7: Values of Selected Design and Operative Variables for CCGT1P - Comparison for Section 5, considering Actual Market Conditions

Variable	Economic Optima, Problem P3	Solution of the Modified Mathematical Formulation, Problem P6	Estimation Error (%)
Costs Ratio	0.2720	0.2720	
Power Demand (MW)	300	300	
Specific Transfer Area (m^2/MW)	254.4	251.2	-1.26
GT Design Power (MW)	216.6	216.9	0.14
ST Design Power (MW)	83.4	83.1	-0.36
Power Plant Production Capacity (MW)	300.0	300.0	0.00
Compression Ratio	15.0	15.0	0.54
Fuel Flow (kmol/seg)	0.685	0.685	0.04
Air Flow (kmol/seg)	23.3	23.3	0.19
HRSG Exchange Area (m^2)	67660	66732	-1.37
Economizer Area Fraction (%)	30.6	30.5	-0.50
Evaporator Area Fraction (%)	61.7	61.8	0.19
Superheater Area Fraction (%)	7.6	7.7	0.50
Operative Pressure (atm)	29	29	0.43
Thermal Efficiency (%)	52.66	52.64	-0.04
Total Annual Cost (M$/MW)	0.0837	0.0838	0.03

Table 8

Table 8: Values of Selected Design and Operative Variables for CCGT3P - Comparison for Section 5, considering Actual Market Conditions

Variable		Economic Optima, Problem P3	Solution of the Modified Mathematical Formulation, Problem P6	Estimation Error (%)
Costs Ratio		0.2720	0.2720	
Power Demand (MW)		1000	1000	
Specific Transfer Area (m^2/MW)		476.9	475.6	-0.27
GT Design Power (MW)		341.3	341.5	0.05
ST Design Power (MW)		317.4	317.0	-0.11
Power Plant Production Capacity (MW)		1000.0	1000.0	0.00
Compression Ratio		29.7	29.6	-0.07
Fuel Flow (kmol/seg)		0.911	0.912	0.08
Air Flow (kmol/seg)		21.1	21.1	0.11
HRSG Exchange Area (m^2)		230687	230096	-0.26
Deaerator Section	Exchange Area (m^2)	30072	30145	0.24
	Economizer Area Fraction (%)	49.3	49.5	0.28
	Evaporator Area Fraction (%)	50.7	50.5	-0.28
	Operative Pressure (atm)	1.4	1.4	0.36
Low Pressure	Exchange Area (m^2)	21730	21783	0.24
	Economizer Area Fraction	0.9	0.8	-0.69

Section	(%)			
	Evaporator Area Fraction (%)	82.5	82.4	-0.10
	Superheater Area Fraction (%)	16.7	16.8	0.51
	Operative Pressure (atm)	2.8	2.8	0.36
Intermediate Pressure Section	Exchange Area (m^2)	57638	57779	0.24
	Economizer Area Fraction (%)	10.9	10.9	0.51
	Evaporator Area Fraction (%)	70.0	70.0	-0.04
	Superheater Area Fraction (%)	19.1	19.1	-0.13
	Operative Pressure (atm)	8.3	8.3	0.36
High Pressure Section	Exchange Area (m^2)	111285	110502	-0.70
	Economizer Area Fraction (%)	44.9	44.8	-0.13
	Evaporator Area Fraction (%)	33.2	33.3	0.50
	Superheater Area Fraction (%)	21.9	21.8	-0.50
	Operative Pressure (atm)	97.7	98.6	0.91
Reheater Section	Exchange Area (m^2)	9962	9887	-0.75
	Operative Pressure (atm)	97.7	98.6	0.91
Thermal Efficiency (%)		66.02	65.96	-0.08

Total Annual Cost (M$/MW)	0.0721	0.0721	0.05

Table 9

Table 9: Values of Selected Design and Operative Variables for CCGT3P - Comparison for Section 5, considering Plant Economics Dominated by Cost of Investment on Transfer Area

Variable		Economic Optima, Problem P3	Solution of the Modified Mathematical Formulation, Problem P6	Estimation Error (%)
Costs Ratio		0.001088	0.001088	
Power Demand (MW)		1000	1000	
Specific Transfer Area (m^2/MW)		310.0	311.2	0.39
GT Design Power (MW)		344.9	344.9	0.00
ST Design Power (MW)		310.2	310.2	0.00
Power Plant Production Capacity (MW)		1000.0	1000.0	0.00
Compression Ratio		30.0	30.0	0.00
Fuel Flow (kmol/seg)		0.937	0.937	0.00
Air Flow (kmol/seg)		21.3	21.3	0.00
HRSG Exchange Area (m^2)		146794	147483	0.47
Deaerator Section	Exchange Area (m^2)	38409	38420	0.03
	Economizer Area Fraction (%)	32.1	32.1	0.03
	Evaporator Area Fraction (%)	67.9	67.9	-0.02
	Operative Pressure (atm)	1.4	1.4	0.45
Low Pressure	Exchange Area (m^2)	19513	19703	0.97
	Economizer Area Fraction	1.3	1.3	-0.50

Section	(%)			
	Evaporator Area Fraction (%)	97.3	97.4	0.01
	Superheater Area Fraction (%)	1.4	1.3	-0.50
	Operative Pressure (atm)	2.8	2.8	0.52
Intermediate Pressure Section	Exchange Area (m^2)	23277	23503	0.97
	Economizer Area Fraction (%)	7.7	7.7	-0.27
	Evaporator Area Fraction (%)	81.4	81.5	0.06
	Superheater Area Fraction (%)	10.9	10.9	-0.26
	Operative Pressure (atm)	8.4	8.5	0.52
High Pressure Section	Exchange Area (m^2)	57295	57477	0.32
	Economizer Area Fraction (%)	41.9	42.1	0.37
	Evaporator Area Fraction (%)	50.7	50.5	-0.37
	Superheater Area Fraction (%)	7.3	7.4	0.39
	Operative Pressure (atm)	50.5	50.8	0.52
Reheater Section	Exchange Area (m^2)	8300	8380	0.97
	Operative Pressure (atm)	50.5	50.8	0.52
Thermal Efficiency (%)		64.15	64.15	0.00

Total Annual Cost (M$/MW)	0.128	0.128	0.10

Table 10

Table 10: Input Data

Item	Symbol	Units	Value
Air Characteristics			
Humidity		%	60
Temperature		K	298
Fuel Characteristics			
Methane Molar Fraction	X_{F,CH_4}	%	91.41
Ethane Molar Fraction	X_{F,C_2H_6}	%	4.73
Propane Molar Fraction	X_{F,C_3H_8}	%	0.83
Butane Molar Fraction	$X_{F,C_4H_{10}}$	%	0.29
Pentane Molar Fraction	$X_{F,C_5H_{12}}$	%	0.09
Hexane Molar Fraction	$X_{F,C_6H_{14}}$	%	0.07
Nitrogen Molar Fraction	X_{F,N_2}	%	0.89
Carbon Dioxide Molar Fraction	X_{F,CO_2}	%	1.69
Pressure	P_F	atm	40
Polytropic Efficiencies			
Air Compressor	$\eta_{AC,p}$	%	92
Gas Turbine	$\eta_{GT,p}$	%	90
Steam Turbine	$\eta_{ST,p}$	%	92
Combustion Chamber Thermal Efficiency			
CC and PCC	η_{COMB}	%	98
Polytropic Index			

Air – AC	kp_{AC}		1.38
Gas – GT1	kp_{GT1}		1.32
Gas – GT2	kp_{GT2}		1.30
Steam – ST LP	$kp_{ST\ LP}$		1.23
Steam – ST IP	$kp_{ST\ IP}$		1.28
Steam – ST HP	$kp_{ST\ HP}$		1.29
Overall Heat Transfer Coefficient			
Overall Coefficient– ECO DEA	$U_{ECO\ DEA}$	kW/m^2 K	0.0505
Overall Coefficient– ECO LP	$U_{ECO\ LP}$	kW/m^2 K	0.0299
Overall Coefficient – ECO1 IP	$U_{ECO1\ IP}$	kW/m^2 K	0.0680
Overall Coefficient – ECO2 IP	$U_{ECO2\ IP}$	kW/m^2 K	0.0525
Overall Coefficient – ECO1 HP	$U_{ECO1\ HP}$	kW/m^2 K	0.0613
Overall Coefficient – ECO2 HP	$U_{ECO2\ HP}$	kW/m^2 K	0.0592
Overall Coefficient – ECO3 HP	$U_{ECO3\ HP}$	kW/m^2 K	0.0552
Overall Coefficient – EVA DEA	$U_{EVA\ DEA}$	kW/m^2 K	0.0093
Overall Coefficient – EVA LP	$U_{EVA\ LP}$	kW/m^2 K	0.0250
Overall Coefficient – EVA IP	$U_{EVA\ IP}$	kW/m^2 K	0.0359
Overall Coefficient – EVA HP	$U_{EVA\ HP}$	kW/m^2 K	0.0527
Overall Coefficient – SH LP	$U_{SH\ LP}$	kW/m^2 K	0.0059
Overall Coefficient – SH1 IP	$U_{SH1\ IP}$	kW/m^2 K	0.0424
Overall Coefficient – SH2 IP	$U_{SH2\ IP}$	kW/m^2 K	0.0314
Overall Coefficient – SH HP	$U_{SH\ HP}$	kW/m^2 K	0.0317
Overall Coefficient – RH	$U_{SH\ RH}$	kW/m^2 K	0.0633

Overall Coefficient – REG	$U_{SH\ REG}$	kW/m^2 K	0.132
Operative Restrictions			
Min Pinch Point	$PinchP_{min}$	K	5
Max Pinch Point	$PinchP_{max}$	K	15
Min Approach Point	$ApproachP_{min}$	K	5
Max Approach Point	$ApproachP_{max}$	K	15
Max Operative Pressure – HP Operative Level	$P_{THP,max}$	atm	110
Max Operative Pressure – IP Operative Level	$P_{TIP,max}$	atm	18.3
Max Operative Pressure – LP Operative Level	$P_{TLP,max}$	atm	6.1
Max Operative Pressure – DEA Operative Level	$P_{TDEA,max}$	atm	3.1
Max Operative Pressure – CON Operative Level	$P_{TCON,max}$	atm	0.15
Min Operative Pressure – CON Operative Level	$P_{TCON,min}$	atm	0.05
Min HRSG Discharge Pressure	$P_{HRSG,min}$	atm	1.005
Max HRSG Inlet Temperature	$T_{HRSG,max}$	K	900
Min HRSG Discharge Temperature	$T_{HRSG,min}$	K	360
Max Turbine Inlet Temperature – GT	$T_{GT,max}$	K	1500
Max Turbine Inlet Temperature –	$T_{ST,max}$	K	850

ST			
Min Temperature Difference at Superheater Exit	$\Delta T_{SH,min}$	K	30
Min Temperature Difference at Condenser Exit	$\Delta T_{CON,min}$	K	4
Min Temperature Difference at Regenerator Exit	$\Delta T_{REG,min}$	K	40
Min Steam Quality – ST	$X_{ST,WSM,min}$		0.92
Max Steam Quality – ST	$X_{ST,WSM,max}$		0.97
Max Compression Ratio	$CR_{PC,max}$		30

Figure 1

Click here to download high resolution image

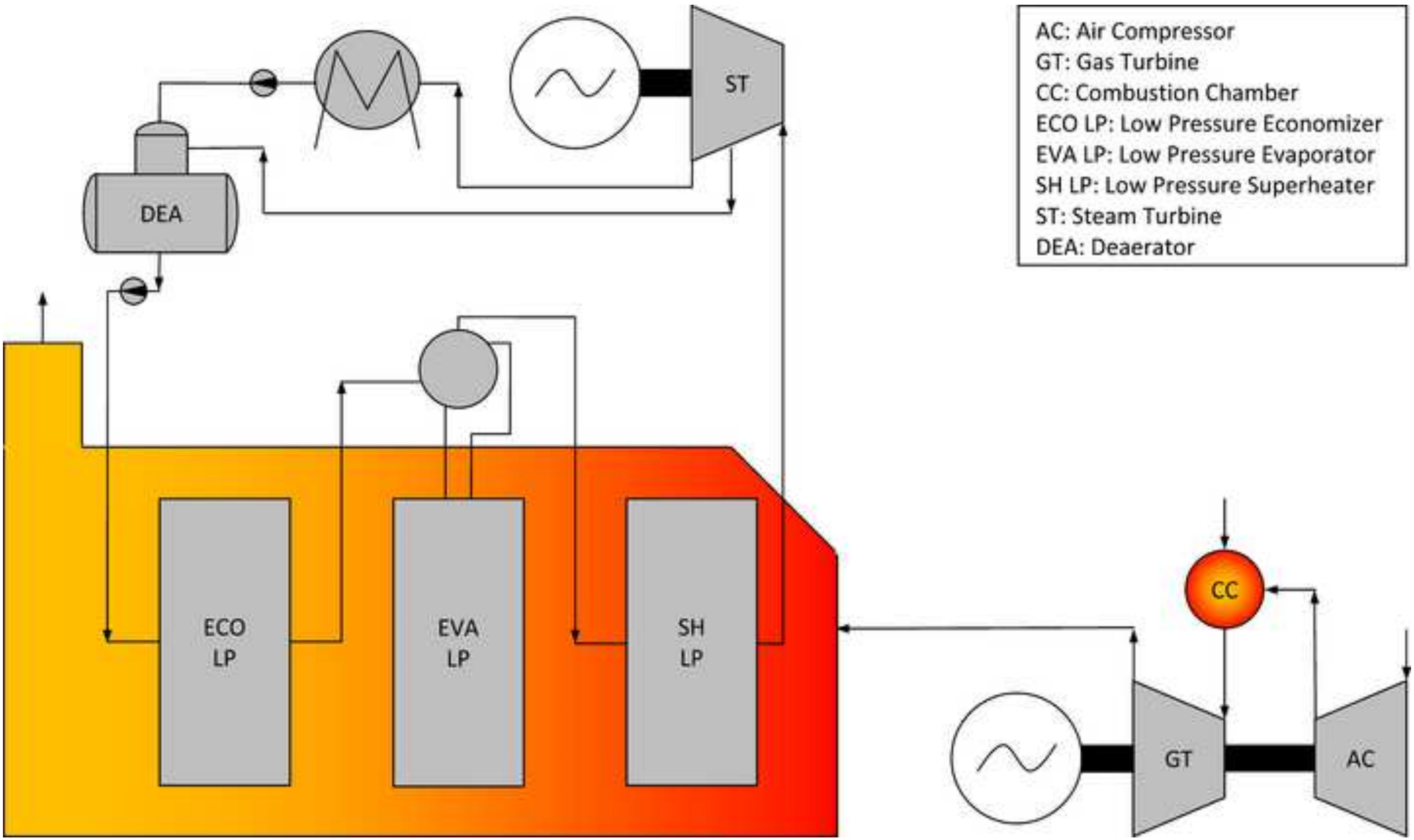

Figure 2
Click here to download high resolution image

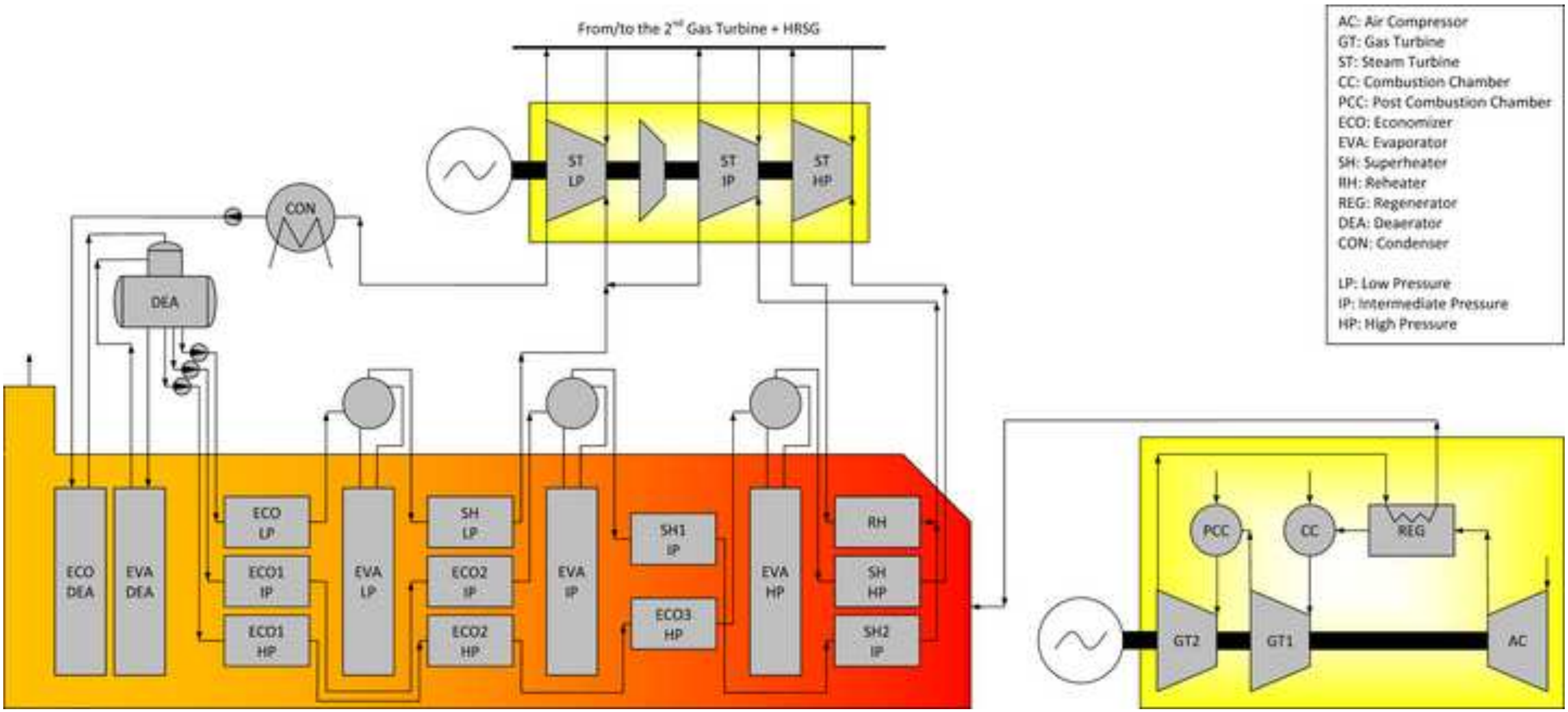

Figure 3
Click here to download high resolution image

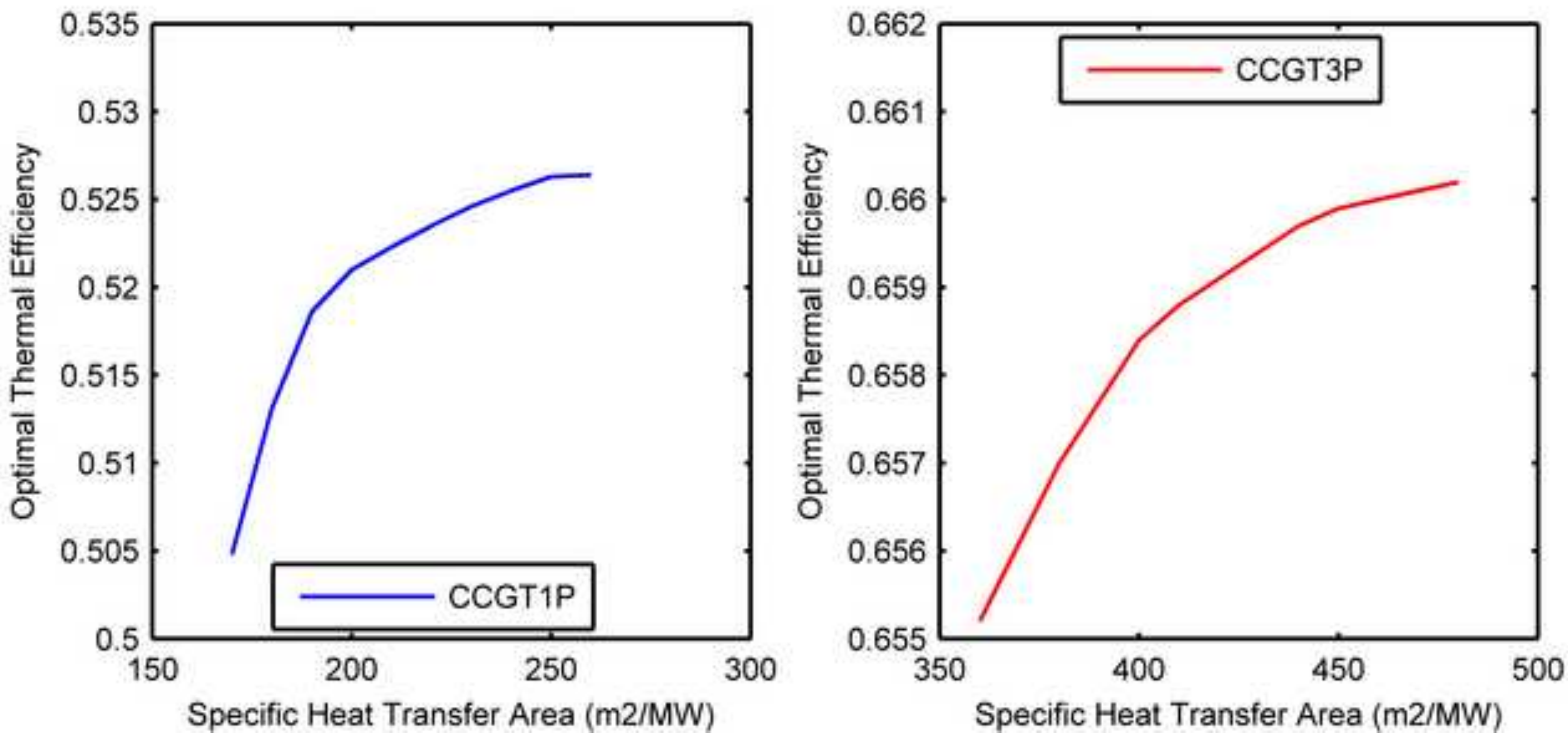

Figure 4
Click here to download high resolution image

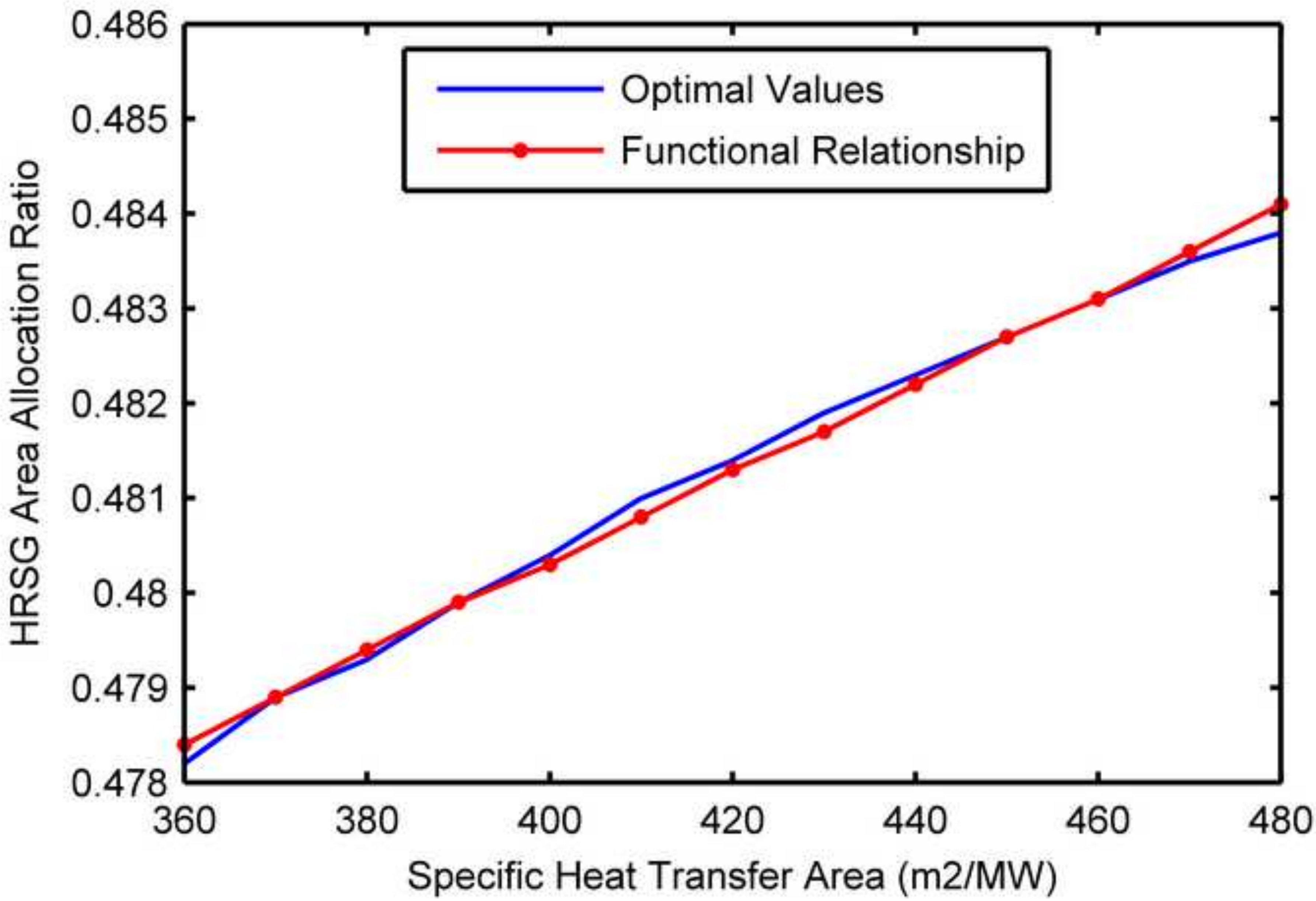

Figure 5
Click here to download high resolution image

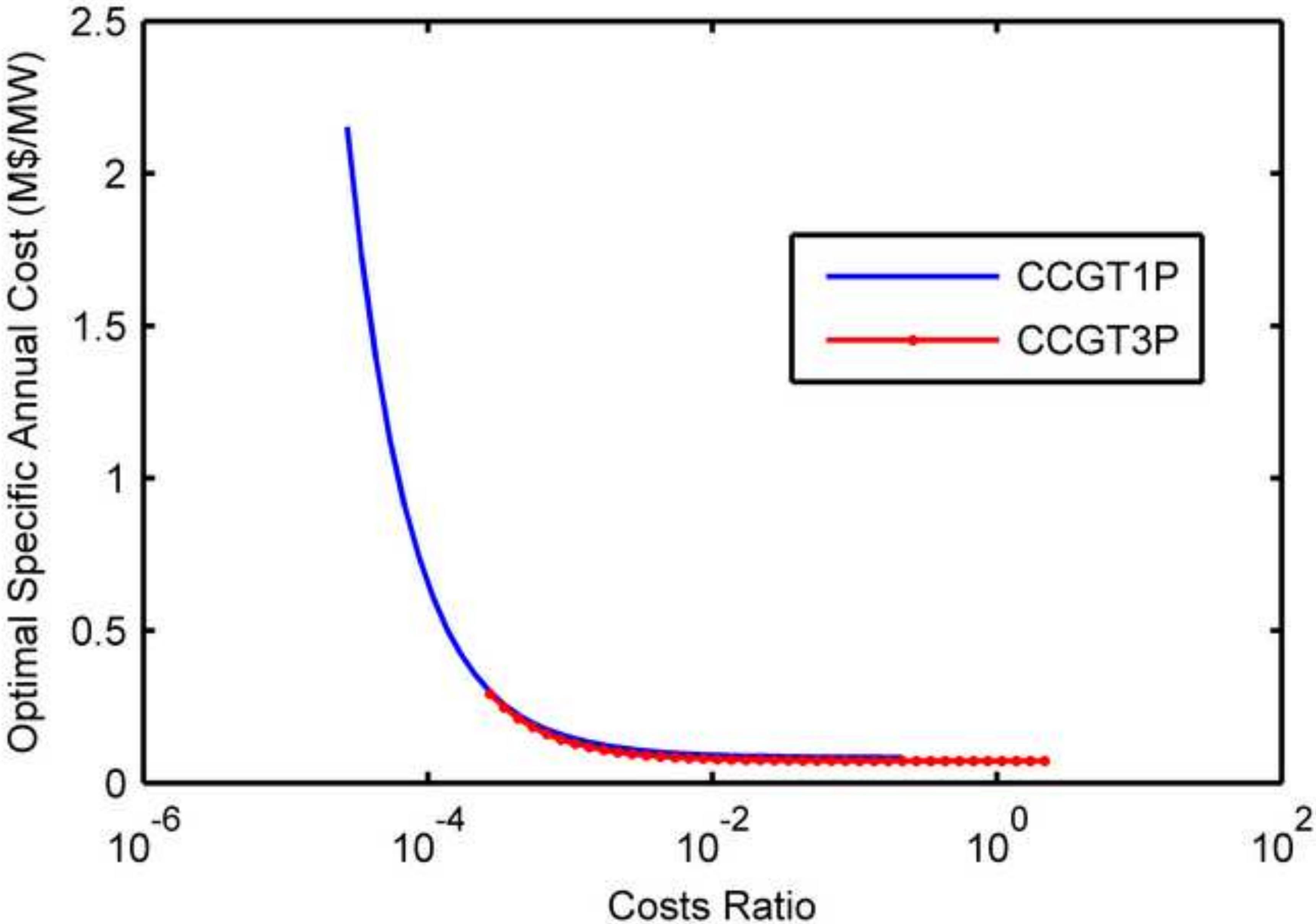

Figure 6
Click here to download high resolution image

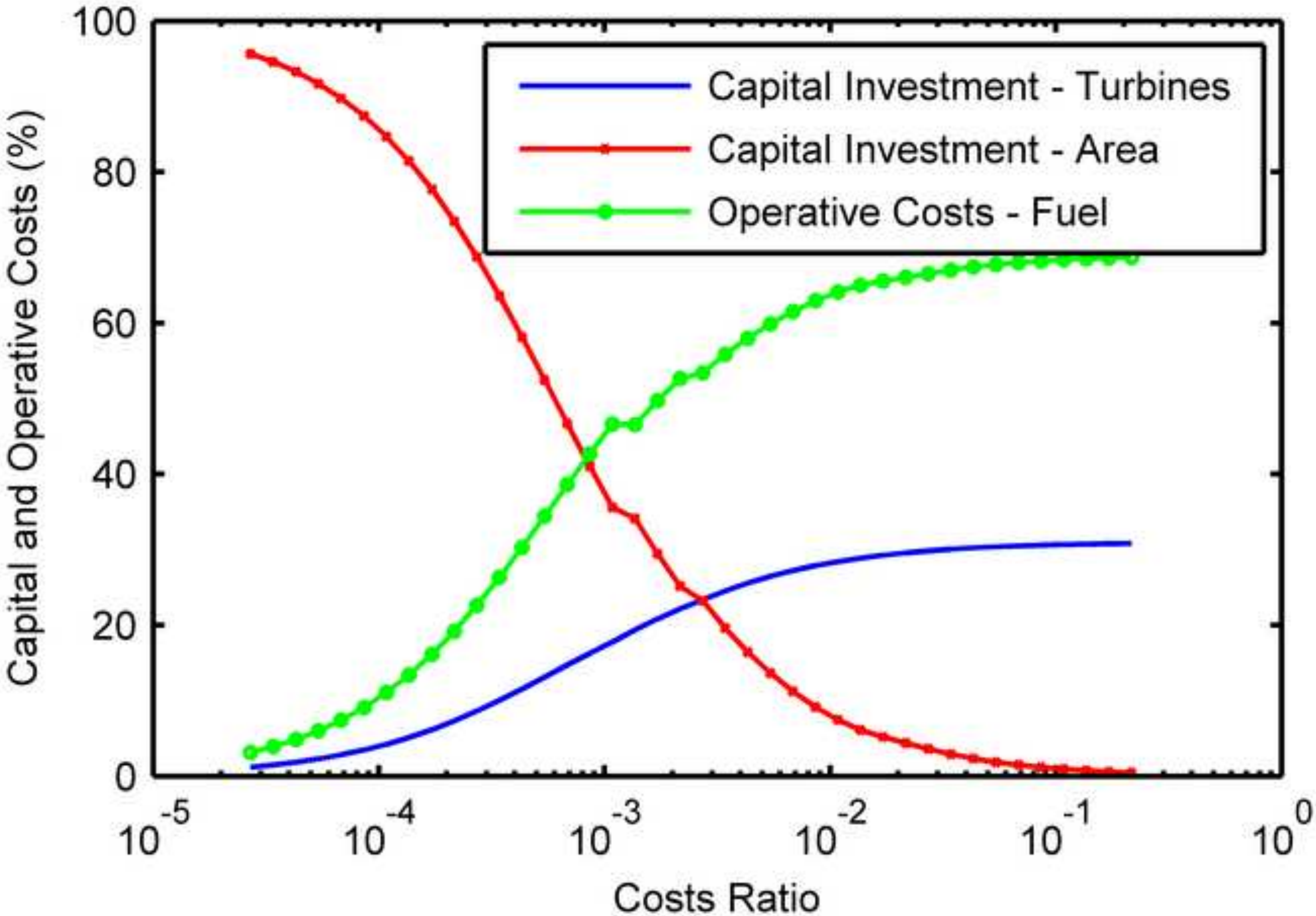

Figure 7

Click here to download high resolution image

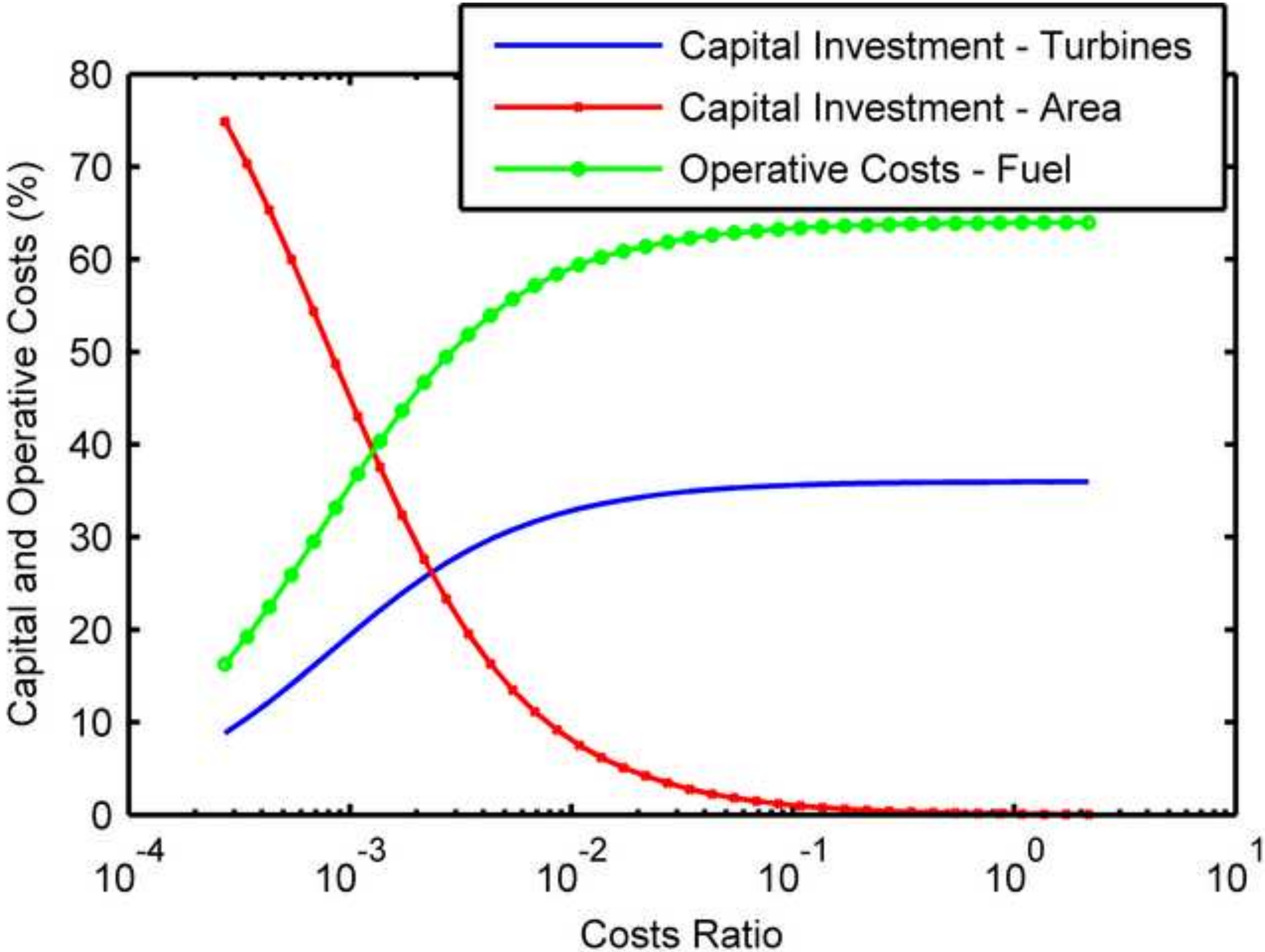

Figure 8

Click here to download high resolution image

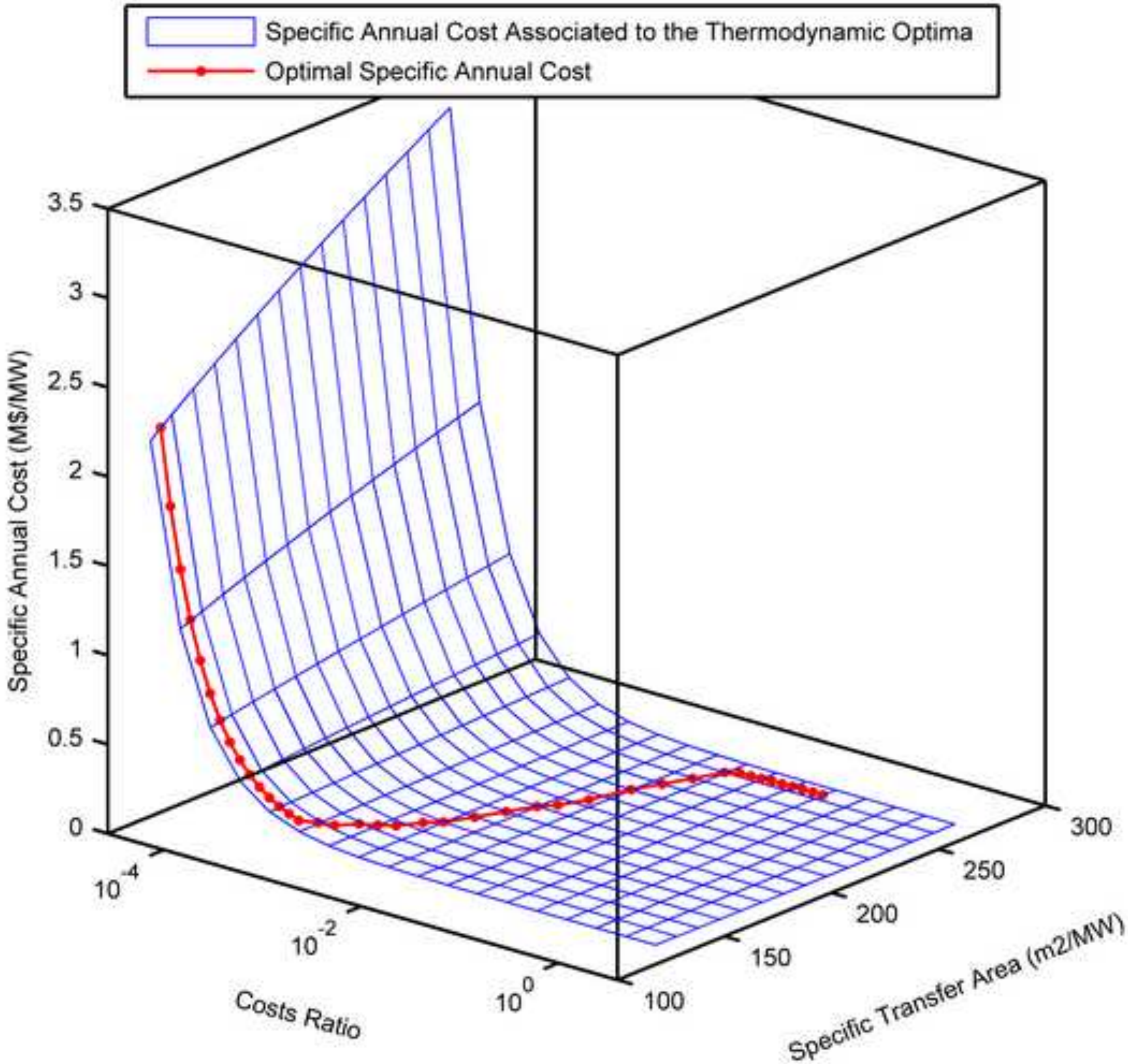

Figure 9
Click here to download high resolution image

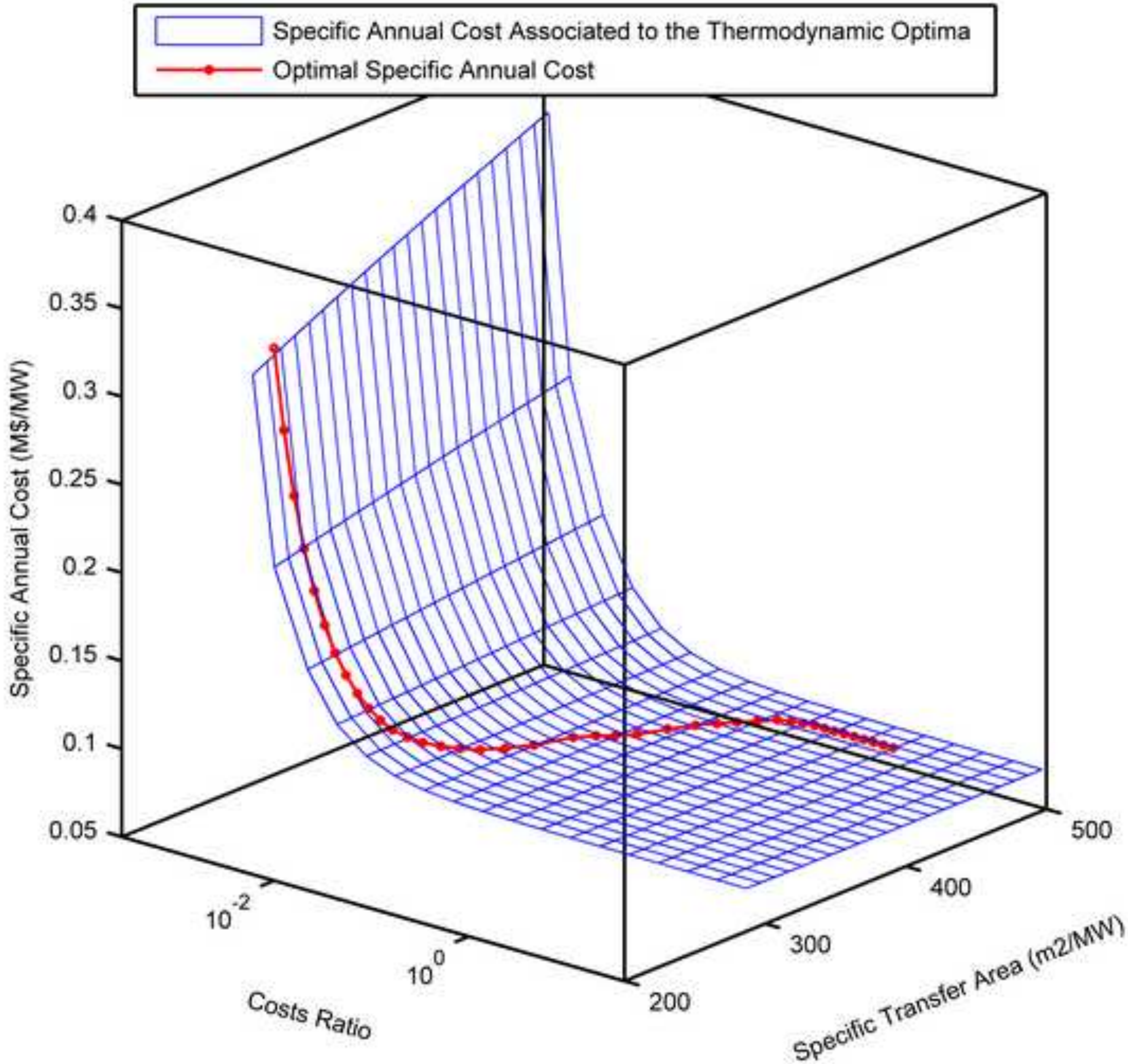

Figure 10
Click here to download high resolution image

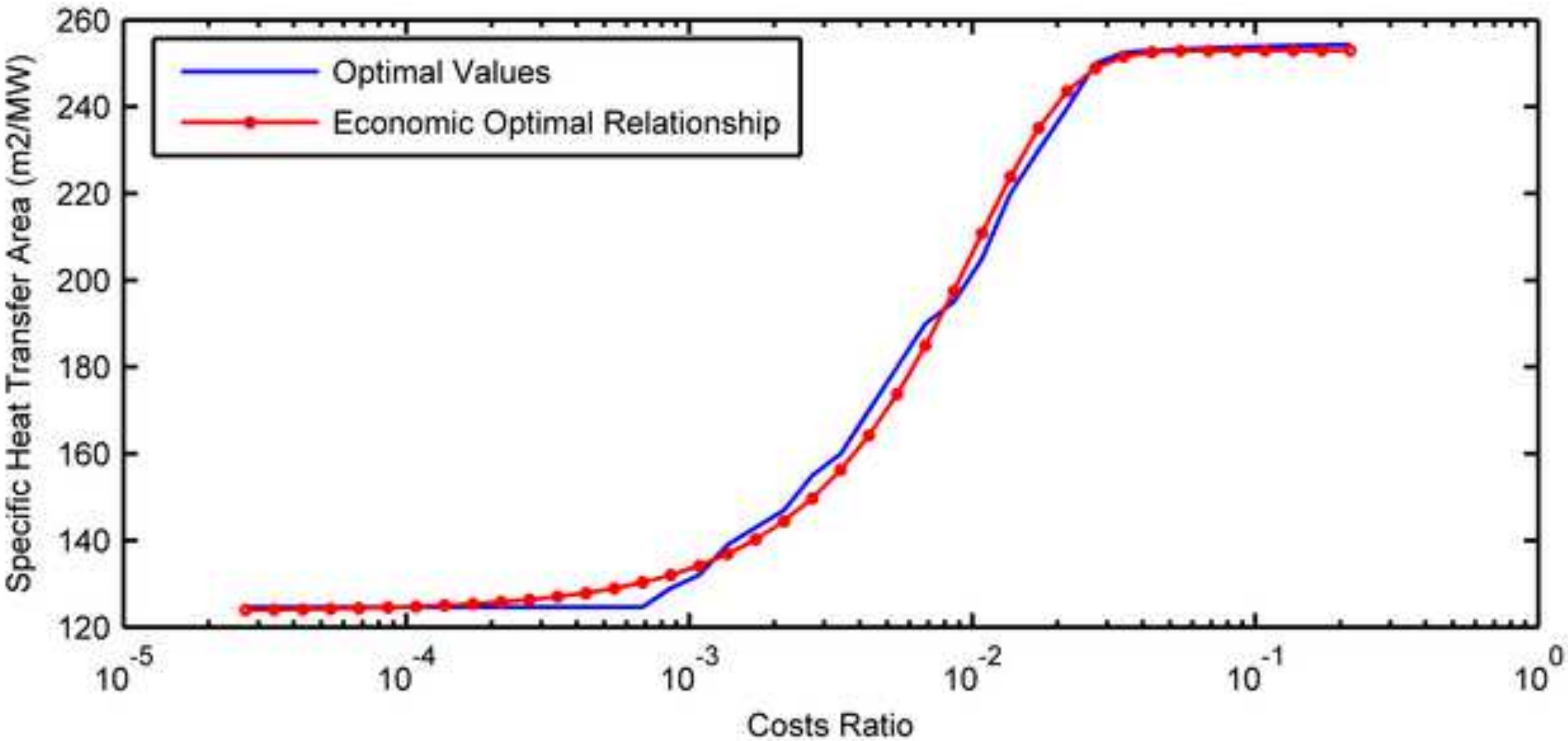

Figure 11
Click here to download high resolution image